# Chapter 1
# Introduction

**Karl H. Schoenbach, Eberhard Neumann, Richard Heller, P. Thomas Vernier, Justin Teissie, and Stephen J. Beebe**

**Abstract** Electroporation, the electropermeabilization of cell membranes, is a basic and most thoroughly studied bioelectric effect caused by pulsed electric fields. Section 1.1 gives a brief introduction into the research history of this effect and revisits the original chemical thermodynamic concept of membrane poration, which was introduced in 1982 in the context of the first electro-genetic reprogramming of cells with foreign DNA. Most of the applications of this effect have since been based on the use of millisecond and microsecond pulses with electric field amplitudes ranging from the upper tens of V/cm to several kV/cm. Section 1.2 provides a brief overview of the history in this important field of research and introduces medical and biotechnological applications, based on reversible and irreversible electropermeabilization with millisecond/microsecond pulses. More recently the pulse duration has been extended into the nanosecond and even picosecond range, with pulsed electric fields ranging from kV/cm to more than 100 kV/cm. The application of such ultrashort pulses has been shown to affect not only the plasma membrane of cells but also subcellular structures. The development of the research in this area and applications of nanosecond and picosecond bioelectric effects are covered in Sect. 1.3.

**Keywords** Electroporation • History of electroporation/electropermeabilization • Millisecond/microsecond pulse effects • Nanosecond/picosecond pulse effects • Medical and biotechnological applications

K.H. Schoenbach (✉) • R. Heller • P.T. Vernier • S.J. Beebe
Old Dominion University, Norfolk, VA, USA
e-mail: kschoenb@odu.edu

E. Neumann
University of Bielefeld, Bielefeld, Germany

J. Teissie
Université de Toulouse and Institute of Pharmacology and Structural Biology, Toulouse, France



H. Akiyama, R. Heller (eds.), *Bioelectrics*, DOI 10.1007/978-4-431-56095-1_1

## 1.1 History of the Membrane Electroporation Concept

Eberhard Neumann

The original chemical thermodynamic concept of membrane electroporation (MEP), introduced in 1982 in the context of the first genetic reprogramming of cells with foreign naked DNA by using electric pulses, is revisited. In addition, an advanced physical chemical analysis of MEP data correlations is outlined in terms of pore density statistics. A new strategy for a stepwise analysis of electroporation data correlations suggests starting with the low-field range, which directly yields the average single-pore polarizability and eventually the pore radii. Further, at a given applied electric field, the induced membrane fields in spheroidal membrane shells are dependent on the angular position. Consequently, experimental quantities, such as the extent of poration and the pore distribution constant, reflect averages of field-dependent cos squared terms. Remarkably, the "in-field" kinetics indicates that the pore density increases in two consecutive steps and includes the delayed Maxwell stress-induced shape changes of membrane shells. Both the rapid in-field kinetic modes and the longer-lasting post-field pore resealing phases indicate that transmembrane fluxes of small ions and larger molecules are coupled to the structural changes modulating the transport. Therefore, flux analysis uses the concept of time-dependent (interaction) flux coefficients to rationalize the characteristic sigmoid onsets and apparently stretched exponentials, qualifying "stretched" as "exponentials of exponentials."

### *1.1.1 Introduction*

When it was found that electric field pulses together with naked foreign gene DNA can be used to genetically reprogram biological cells, the general interest in bioelectric phenomena and electric pulse techniques gained enormous impetus for field-controlled chemical cell manipulations. Historically, the field effect leading to uptake of biogenic agents like DNA was termed membrane "electroporation," short for "electric pore formation," in 1982 [1]. As such, the term electroporation intends to qualify the chemical structural basis for the observed permeability changes for small ions and (even poly-ionic) macromolecules that usually do not penetrate the lipid phase of membranes.

In more detail, the chemical thermodynamic concept for electroporation was already specified in the context of the first electrotransfer of naked foreign DNA into living mouse lyoma cells by the high-voltage pulse trains leading to stable reprogramming of the cell genome [1, 2]. Prior and complementary to functional electro-uptake, it had been found that electric pulses cause electro-release of

cellular components, such as catecholamines, ATP, Ca-ions, and chromogranine proteins from isolated chromaffin granules of bovine adrenal medullae [3].

Similarly, in 1980 it was shown that aggregated dictyostelium cells exposed to a train of electric field pulses, in the post-field time phase, reorganize (facilitated by added Ca-ions) and form viable giant syncytia by (electroporative) cell–cell fusion (electrofusion) [4]. The post-field kinetics is generally slower and covers a longer time range of several seconds. This indicates that the (in-field) induced porous membrane states are (at zero field) structurally long lived as compared to the rapid process of in-field pore formation.

These early field effect data and the electroporation concept have been valued, among others, in Nature Methods [5] as seminal for the various biotechnological and medical applications; among them are the clinical applications of voltage pulses combined with bioactive agents in the clinical discipline of electrochemotherapy and gene electrotransfer. In this context, we appreciate the critical input of members of the laboratories of, initially, L. M. Mir, J. Teissie, M.-P. Rols, D. Miklavcic, G. Sersa, R. Heller, J. C. Weaver, Y. Chizmadzhev, B. Rubinsky, K. H. Schoenbach, I. Tsoneva, and later, U. Pliquett, M. Kotulska, W. Frei, J. Gehl, R. Boeckmann, H. Grubmueller, T. Vernier, M. Tarek, and many others.

It is recalled that the original "thermodynamic concept of membrane electroporation" was only sketched for the overall description of the dependence of the fractional extent of poration (and implicitly the kinetic constants) on the field pulse parameters in terms of pore reaction quantities like induced pore polarization volumes (and eventually pore radius). The present personal review on the early history of membrane electroporation (MEP) is therefore restricted to those selected examples where electroporation data were subjected to rigorous chemical kinetic and chemical thermodynamic analysis.

In the original thermodynamic concept, the mass action law for a two-state structural interaction scheme had been formulated, and the dependence of the chemical state distribution constant on physical state parameters like temperature, pressure, or electric field was given in the differential form of a general Van't Hoff relationship [1]. It is emphasized that, as such, chemical thermodynamics is a general physical chemical approach for the analysis of appropriate data correlations in terms of established thermodynamic laws. Thus, chemical thermodynamics is not an alternative theory competing with other physical theories.

Due to novel single-particle techniques and progress in analytical theory, however, the original thermodynamic approach to MEP has to be substantially refined. In particular, it is realized that the experimental electroporation data of cell ensembles (and thus of electropore ensembles) in homogeneous suspensions are "double-average values" of the polar angular position and of (position dependent) local electric field strength. It is outlined below how the experimental parameters like pore distribution constants and fractional pore densities can be explicitly expressed in terms of positional averages of the (centrosymmetric) electropore reactivity confined to spherical shells with position-dependent local fields. The inclusion of these, so far often disregarded, average aspects and of the field-dependent

"membrane conductivity factor" should resolve obvious discrepancies in data interpretations. For example, the actual data assumed to reflect the fractional increase of the field effect appear to be better described when the exponent of the field parameter is linearly dependent on the electric field strength, $E$. However, the concept of induced polarization (of the pore water) clearly is associated with a square dependence ($E^2$).

### *1.1.2 Ensemble Kinetics of Electroporation*

It is essential that there is a fundamental difference between the rate of opening and closing of a single-pore event, as compared to the chemical kinetics of ensembles of membrane pores. The rate parameters of ensemble kinetics are obtained from the analysis of the entire time-course Sig(t) of an appropriate signal that reflects—either direct or indirect—proportionality to the density of pores. Here, pore density refers to the number of pores in the shell volume of the closed membrane system of a lipid vesicle or a cell.

The access to electric pore formation is usually indirect. It has to be checked whether the observed transport kinetics are rate limited by the structural changes (in the lipid–water interfaces) underlying the statistics of pore opening and closing events. For instance, the time course of forward light scattering (of polarized light) can indicate the entrance of water into the lipid membrane, and also global shape changes concomitant with vesicle volume changes. The time course of conductance parameters can indicate field-induced transmembrane flux of small ions. Spectroscopic methods are used to indirectly monitor membrane transport of larger molecules like optical dyes or dye-labeled DNA.

Here, it is practical to differentiate between "in-field" responses and "post-field" responses like the slower pore ensemble resealing phases. In classical electroporation kinetics, the actual time-course Sig(t) of the respective signal is analyzed in terms of (exponential) normal modes. Each exponential mode is characterized by the relaxation time constant and the mode amplitude. It is shown below that flux analysis requires "time-dependent rate coefficients."

In particular, the relaxation kinetic data of unilamellar lipid vesicles [6] and of densely packed CHO cells [7] are instrumental for elucidating the mechanism of pore formation. Already the actual time courses of poration events show peculiarities such as delayed parallel modes. In the low-field strength range, pore formation is roughly mono-exponential with time. The (field-dependent) relaxation times are in the range of 5 μs (low field) down to about 0.5 μs (high field). The post-field relaxation covers a longer time range (stretched exponentials); the "zero-field" time constants are in the range of 1 ms to 10 ms. Even if the ion concentration outside is much smaller than the inside concentration, the post-field response indicates no net transport of ions to the outside. So, the pores are conductive but do not indicate measurable net outflux. These "rapid" pores appear to be permselective either for single file cation flux or for single file anion flux; they are thus associated with local

Nernst potentials counteracting the field-induced potentials. They were called type-1 pores (P1), estimated average pore radius of $0.5 \pm 0.2$ nm.

At field strengths higher than a "threshold field strength," the initial exponential phase (of P1 pores) appears to saturate, and at about 5 μs the signal slowly increases. At about 5 μs, a delayed second transport mode appears. The delay is particularly pronounced when adsorbed macromolecules are present or when shape changes due to Maxwell stress lead to net outflux of intra-particle salt solution. This special feature suggests that a second type of larger pores is formed at the expense of P1 pores. The in-field time constants for the P2 pores are estimated to be in the range of 100–30 μs, estimated pore radius of about $1.0 \pm 0.2$ nm. The post-field response is extremely stretched and can cover the time range of 10–100 ms and even several seconds [7]. In the case of voltage clamp (i.e., the membrane field is forced to be constant), ion fluxes do not reduce the transmembrane field and pores may expand up to pore radii of 10 nm and more [8–12]. In both cases, structural longevity of pore ensembles at zero field underlies (and rationalizes) the large post-field membrane transport. This is particularly apparent when the unavoidable adsorption of (macro) molecules leads to prolonged membrane insertion and thus to delayed (zero-field) dissociation from the membrane. In addition, at higher field strengths, electromechanical Maxwell stress leads to elongation of lipid vesicles and cells in the field direction and to release of intracellular liquid. Adsorbed molecules facilitate, by curvature effects, both electroporation and material transport as well as shape changes.

In brief, the thermodynamic ensemble approach provides a comprehensive formalism for quantitative analysis and characterization of electroporation data of cells and tissue. Together with results obtained from flux analysis, using the concept of time-dependent flux coefficients, the thermodynamic and kinetic information provides not only a general guideline for the analysis of data correlations but also for the goal-directed design of experiments and apparatus for the various biotechnological and medical electroporation treatments.

### *1.1.3 Molecular Chemical Schemes for Pore Formation*

The chemical electro-thermodynamic concept of membrane electroporation (MEP) views the primary effect of the induced membrane electric field as directly acting on the interface between bulk water and the hydrated polar head groups of lipids, leading to the formation of hydrophobic and hydrophilic pores. The chemical process may be viewed as field-induced cooperative rearrangements of n lipids $L_{aq}$ (hydrated polar head *groups*). *Thereby aqueous pores* $L_n$ and $L_n(W)$ are formed by water ($W$) entrance., according to

$$nL_{aq} \rightleftarrows \left(\mathrm{L}_{aq}\right)_n \overset{+W}{\rightleftharpoons} \left(L_{aq}\right)_n (W) \tag{1.1}$$

The water in the cluster-like configuration $(L_{aq})_n$ $(W)$ is polarized stronger in the induced transmembrane field $(E_m)$ as compared to the smaller field E in the bulk water. Therefore, water entrance into the higher electric field of the membrane site contributes strongly to the thermodynamic stability of small aqueous hydrophobic (*HO*) and larger hydrophilic (*HI*) or inverted pores [13]. The observed longevity (larger pore life times) of the ensemble of local pore structures is due to the local cooperativity of the ordered lipids in the highly curved pore wall of a hydrophilic pore. The steps from the closed membrane sites $(L_{aq})_n$ (denoted *C*) to the various pore states had been cast in the scheme: C $\rightleftarrows$ HO $\rightleftharpoons$ HI.

Field-induced rotational motions of the polar lipids in the curved pore wall (of the *HI* pore) also rationalize the huge acceleration of lipid flip-flop and other intra-wall motions such as the translocation of phosphoryl inositol from the internal membrane monolayer to the outer monolayer. Electric pulses of low-field intensity but longer pulse duration facilitate, via electroporation, both endocytotic uptake of external particles and exocytotic release of intracellular components.

The structural feature of pore longevity is also instrumental for rationalizing some of the voltage pulse data for pulse train combination modes of high-voltage (HV) pulses and low-voltage (LV) pulses and the effects of a time interval between the pulses [14]. Viewed afterward, the originally applied "exponential field pulses" [1, 2], with the longer RC-circuit discharge times, combine the HV part of the initial time course with the LV part of the slower part.

As compared to the chemical thermodynamic approach, it appears that the majority of detailed (physical) electroporation theories primarily address the physical aspects like the electric polarization term of pore water, pore line tension, and membrane surface tension, membrane curvature and bending rigidity, and other factors in terms of "pore radius." They do not explicitly address the chemical free energy changes of rearrangements of the lipids and water in pore wall formation and pore resealing.

### *1.1.4 Global Electroporation Scheme*

In order to understand the electroporation phenomena on the membrane level, it is essential to recall that an electric field (of a voltage pulse) acts (here via the larger induced membrane field) as a force on chemical structures, vectorial and simultaneously on all polar (ionic and dipolar) groups of the membrane components. Note, the induced membrane field originates from the mobile ions near the two surface sides of the dielectric membrane (Maxwell–Wagner ionic polarization). When macromolecules adsorb on the membrane surface, the adsorption complex necessarily is situated within the induced field across the "complex."

It is common experience that cellular electroporation data correlations can be satisfactory rationalized in terms of a global overall scheme for the structural transitions of pore formation and pore resealing viewed as cascades of field-sensitive closed membrane states ($C$) and a sequence of porous states ($P$):

$$(C) \overset{+W}{\rightleftharpoons} (P) \rightarrow X(Sig) \tag{1.2}$$

In scheme (1.2), the term $X(Sig)$ is to indicate that the preceding structural transition is necessarily coupled to transport phenomena and transport feeds back to the extent of transition. The transport of small ion fluxes leads to reduction of the induced transmembrane field; this reduces the extent of poration even if the external field remains constant. Under the special condition of low external salt concentration, oscillations in the membrane field and in the global shape are observed [12].

The thermodynamic overall distribution constant $K_p\,(E)$ for the overall two-state scheme is defined as

$$K_p(E) = \frac{[P]}{[C]} = \frac{[P]}{[P]_{\max} - [P]} = \frac{f_p}{1 - f_p} \tag{1.3}$$

The thermodynamic field dependence is denoted by $K_p\,(E)$. The state density of potential pore sites is given by $[\mathrm{C}] = [\mathrm{P}]_{\max} - [\mathrm{P}]$, where the maximum value $[P]$ max (at field infinity) is used as a reference for the pore state density $[P]$. The overall fraction of pore states is given by

$$f_p(E) = \frac{[\mathrm{P}]}{[\mathrm{P}]_{\max}} = \frac{K_p(E)}{1 + K_p(E)} \tag{1.4}$$

The numerical value of $f_p\,(E)$ is limited to the range $0 \leq f_p \leq 1$. (The previous restricted assumption of $K \ll 1$, reducing Eq. (1.4) to $\mathrm{f_p(E)} = \mathrm{K_p(E)}$, is justified only for the low-field range [6, 7].) The analysis of the field dependence of $f_p\,(E)$ requires to first express the fractional extent of poration as $f_p\,(E_m)$, i.e., in terms of the induced local membrane field $E_m$.

### *1.1.5 Chemical Energetics of Field Effects*

The various poration phenomena are thermodynamically rationalized in differential form as dependence of $K_p$ on the generalized thermodynamic forces in terms of a generalized Van't Hoff relationship (1.1). The total differential d ln $K(p,T,E)$ is expressed as partial change $dT$ in the Kelvin temperature $T$, partial change $d$p in the pressure p, and partial change $dE_m$ in the electric field strength $E_m$ of the "locally active" electric field induced by the external applied field E. For a two-state

structural equilibrium transition, Eq. (1.2), the general thermodynamic expression reads

$$RT\ d\ell nK(p,\ T,\ E) = \Delta_r H^o_{p,T}\ dt - \Delta_r V^o_{\mathrm{E},T}\ dp + \Delta_{\mathrm{r}} M^o_{p,T}\ dE_m \tag{1.5}$$

In Eq. (1.5), $R = k_B N_A$ is the gas constant, $k_B$ the Boltzmann constant, and $N_A$ the Loschmidt–Avogadro constant. Equation 1.5 covers the overall electroporation process in terms of the standard value $\Delta_r M^0 = M^0(P) - M^0(C)$ of the (molar) reaction dipole moment, "sonoporation" with the standard value of the reaction volume $\Delta_r V^0$, and "thermo-poration" and thermal aspects of laser "opto-poration" with the standard reaction enthalpy $\Delta_r H^0$. The standard value of the total molar reaction energy is $\Delta_r H^0(E_m) = \Delta_r G^0(E_m) + T\Delta_r S^0(E_m)$ and includes the standard value $\Delta_r G^0(E_m)$ of the reversible work potential and the standard value $\Delta_r S^0(E_m)$ of the molar reaction entropy at constant $p$,$T$.

The field effect distribution constant $K_p\,(E_m)$ is determined by the standard value of the Legendre-transformed Gibbs reaction energy $\Delta_r \hat{G}^0(E_m)$ in the field $E_m$. Using the transformation definition $\hat{G}\,(E_m) = G(0) - E_m M$, where G(0) is the ordinary Gibbs reaction energy (at $E = 0$) and M the projection of the total electric moment vector $\boldsymbol{M}$ onto the direction of the external field vector $\boldsymbol{E}$, the standard value is expressed as

$$\Delta_r \hat{G}^{\,0}(E_m) = \Delta_r G^0(0) - E_m \Delta_r M^0$$

Hence, in terms of the induced local field $E_m$ at constant $p$,$T$, Eq. (1.5) is specified by

$$d\ell nK_p(E_m)/dE_m = \Delta_r M^0_{pp}/RT = \left\langle \Delta_r m_{pp} \right\rangle / k_B T \tag{1.6}$$

In Eq. (1.6), $\left\langle \Delta_r m_{pp} \right\rangle = \Delta_r M^0_{pp}/N_A$ is the average "molecular reaction moment." For field-induced polarization, it is given by $\left\langle \Delta_r m_{pp} \right\rangle = \left\langle \Delta_r \alpha_{pp} \right\rangle E_m$, where the reaction pore polarizability can be expressed as $\langle \Delta_r \alpha_{pp} \rangle = \nu_{pp} \varepsilon_0 (\varepsilon_{pp} - \varepsilon_{lip}), \varepsilon_0$ being the dielectric permittivity of the vacuum. The "pore polarization volume" $v_{pp}$ includes the pore wall and the aqueous inner part. The dielectric term is an effective dielectric constant (order of 50) for the pore volume $v_{pp}$, and $\varepsilon_{lip}$ (=2.3) is the dielectric constant of the lipid phase.

The cylindrical pore polarization model specifies the pore polarization volume as $\nu_{pp} = d_m \pi\, r^2_{\mathrm{out}}$ with the membrane thickness $d_m = 5$ nm and the "outer pore radius" $r_{\mathrm{out}}$. The inner ring radius $r_{\mathrm{in}}$ specifies the aqueous volume as $\nu_{aq} = d_m \pi\, r^2_{in}$; thus the volume of the pore wall ring is $\nu_{pw} = d_m \pi (r^2_{\mathrm{out}} - r^2_{\mathrm{in}})$. Integration of Eq. (1.6) in the limits $E_m = 0$ and $E_m$, yields

$$K_p(E_m) = K_0 \exp[\langle \Delta\alpha_{pp} \rangle E_m^2 / 2k_B T] \tag{1.7}$$

In Eq. (1.7), $K_0 = K_p$ $(E = 0)$ is the apparent distribution constant for occasional fluctuative pore opening–closing events at zero-applied field. Usually $K_0$ is in the order of $10^{-4}$ or even smaller. At zero-applied field, $K_0 = f_0/(1 - f_0)$ refers to the zero-field fraction $f_0 = f_p(E = 0)$ of fluctuative pore events. In living cells $f_0$ is finite due to the membrane potential. Because of the very small values of $K_0$, we may use the approximation $f_0 = K_0$. It is outlined below that the primary parameter obtained from thermodynamic data analysis is the "θ - average reaction polarizability" $\langle \Delta_r \alpha_{pp} \rangle$.

### 1.1.6 The Induced Potential Difference

The data of classical lipid membrane electroporation suggest that the externally applied electric field E induces the larger membrane field $E_m$ that, in turn, "operates" on the membrane structures. Obviously, $E_m$ is parallel to $E$, and in spherical membrane shells, the curvature conditions the asymmetry of the field effect on the lipid head groups, different on the anode side and the cathode side.

For porated membranes, the local induced field $E_m$ determines the current density vector $j_m$ for the cross-membrane ion fluxes (of both, the cations and the anions): $j_m = \lambda_m(-\nabla\varphi_m) = \lambda_m E_m$, where $\lambda_m$ is the conductivity of the membrane (referring to all conductive pores). Because of continuous misconceptions in the literature, some further details have to be refined. In brief, for spherical membrane shells in conductive media, after rapid buildup of both, the ion concentration polarization and the interfacial charge separation polarization (Maxwell-Wagner), the *stationary value* $\Delta\varphi_{\text{ind}}(\theta, E)_{ss}$ of the polarization buildup kinetics $\Delta\varphi_{\text{ind}}(t) = \Delta\varphi_{ind}(\theta, E)_{ss}(1 - \exp[-t/\tau_{pol}])$ at the polar angle $\theta$ to the direction of the external field $E$ (Fig. 1.1) is given by

$$\Delta\varphi_{\text{ind}}(\theta, E_m)_{ss} = -g \cdot a \cdot E \cdot f_\lambda |\cos\theta| \tag{1.8}$$

In Eq. (1.8), $a = a_{out}$ is the outer radius of the spherical membrane shell. The inner radius is given by $a_{in} = a – d_m$, membrane thickness $d_m$. Note, the polar angle for spherical geometry is confined to the range $0° \leq \theta \leq 180°$ (or $0 \leq \theta \leq \pi$), thus $1 \geq |\cos\theta| \geq 0$. For ultra-short pulses (ps, ns) or for the high frequency range (>10 Hz) of a.c. pulses, the Maxwell-Wagner limit of $g = 3/2$ applies. For short pulses (μs, ms and longer) or for the low frequency range of a.c. pulses, the Dukhin g-term $g(Du)$ applies. This term contains the Dukhin factor, which for spherical particles is given by $Du_{sp} = \lambda_{surf}/a_{sp}\,\lambda_{sx}$, where $a_{sp}$ is the outer particle radius, $\lambda_{surf} \approx 1\text{-}3 \times 10^{-9}$ S the surface conductance (linear surface conductivity of O'Konski) and $\lambda_{ex}$ the medium conductivity. The $g(Du)$ term thus accounts for the coupling of the polarization ion fluxes to the ionic content of the suspending medium.

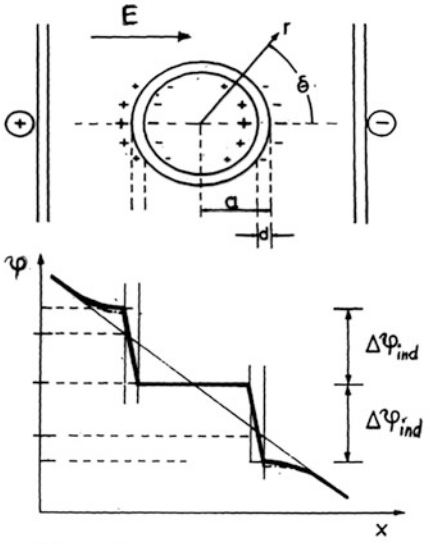


$$\vec{E} = -\vec{\nabla}\varphi\,,\ \Delta\varphi_{ind} = -Ff_{\lambda}(E\cdot a)$$

$$\Delta\varphi_{ind}^{\Theta} = -\frac{3}{2}E\cdot a\cdot f_{\lambda}\cdot|\cos\Theta|$$

$$E_{m}^{\Theta} = -\frac{\Delta\varphi_{ind}^{\Theta}}{d} = \frac{3}{2}\cdot\frac{a}{d}\cdot E\cdot f_{\lambda}\cdot|\cos\Theta|$$

$$f_{\lambda} = 1-\lambda_{m}\cdot\frac{a}{2d\lambda_{ex}} \qquad (\lambda_{in} >> \lambda_{ex})$$

**Fig. 1.1** Scheme for the membrane field amplification by interfacial charge separation polarization (Maxwell–Wagner). Cross section through the center point of the spherical shell (centrosymmetric case) of outer radius $r = a$. The electric potential $\varphi(x)$ through the center point as a function of the x-coordinate for the presence of the dielectric sphere as compared to the absence of the object. The field-induced potential differences $\Delta\varphi_{ind}$ are indicated for the anode (*left*) membrane side and for the cathode (*right*) side. The field amplification by the ratio ($a/d_m$) is specified for the purely dielectric case of $F = g = 3/2$. For the anionic cell wall structures of bacteria and yeast cells and other walled cells (glycocalix shells of up to 200 nm thickness), the Dukhin g-term, $g(Du)$, applies. Note, at finite ionic strength, $g(Du) < 3/2$; see the text

Further, the validity of Eq. (1.8) is restricted to larger objects like cells ($d_m \ll a$) and to very low membrane conductivity $\lambda_m$, i.e., $\lambda_m \ll \lambda_{ex}$, $\lambda_{in}$, where $\lambda_{ex}$ is the external medium conductivity and $\lambda_{in}$ the conductivity of the cell interior. For this case, the conductivity factor for spherical shells in ionic media reduces to [9, 15, 16]

$$f_{\lambda} = 1 - \lambda_m \frac{2\lambda_{ex} + \lambda_{in}}{2\lambda_{ex}\lambda_{in} d_m/a} \tag{1.9}$$

Note that Eq. (1.8) is consistent with the Maxwell definition of the vector **E** as the negative gradient ($E = -\nabla\varphi$) of the electric potential φ. Since the induced

membrane potentials are dependent on position, experimental ensemble properties of spherical shells reflect averages of the contributions of all ring positions (i.e., all polar angles $\theta$ of the spherical shell).

The induced membrane field $E_m(\theta)$ at the polar angle $\theta$ in the direction of **E** (Cartesian coordinate system) is given in terms of membrane voltage $U_m(\theta) = -\Delta\varphi(\theta)$ by

$$E_m(\theta) = \frac{U_m(\theta)}{d_m} = \frac{-\Delta\varphi(\theta)}{d_m} = E_m(0)|\cos\theta| \tag{1.10}$$

In Eq. (1.10), $E_m(0)$ is the (maximum) membrane field at the pole caps at $\theta = 0°$ and at 180°. In the (required) notation of the absolute $|\cos\theta|$, there is no change in sign when going from the "cathode" pole cap, in the range $1 \leq \cos\theta \leq 0$, to the anode one in the angular range $0 \geq \cos\theta \geq (-1)$. Hence Eq. (1.10) is unrestrictive, i.e., generally applicable for the description of current flows *in the direction* of the respective E vector, through the two electroporated hemispheres of a spherical membrane shell in an external field.

### *1.1.7 Contribution of Natural Membrane Potential*

Living cell membranes have a finite natural membrane potential (difference) $\Delta\varphi_{\text{nat}}$. In electrophysiology, the membrane potential is defined as $\Delta\varphi = \varphi(i) - \varphi(\text{o})$, where the outside potential is taken as the reference $\varphi(\text{o}) = 0$. In many cells, the membrane potential is dominated by the Nernst potential $\Delta\varphi(K^+)$ for $K^+$-ions. Due to the dominant contribution of permselectivity for $K^+$, we may use the approximation $\Delta\varphi_{\text{nat}} = \Delta\varphi\ (K^+)$. Typically, $\Delta\varphi_{\text{nat}} = -70$ mV. The contribution to $\Delta\varphi_m$ of the natural membrane potential (difference) $\Delta\varphi_{\text{nat}}$ is readily incorporated. Due to the natural law of additivity of electric potentials, the total term $\Delta\varphi_{\text{m}}$ (θ) at the angular ring position θ is given by $\Delta\varphi_m(\theta) = \Delta\varphi_{\text{ind}}(\theta,E)_{ss} - \Delta\varphi_{nat}\Delta\ sgn(\cos\theta)$, where *sg* $n(\cos\theta) = \cos\theta/|\cos\theta| = \pm 1$ is the sign of cos $\theta$. Note, $\Delta\varphi_{\text{nat}}$ is independent of the angle $\theta$ *(and of E)*.

Insertion of Eq. (1.8) yields [16]

$$\Delta\varphi_m(\theta) = -g \cdot a \cdot E \cdot f_\lambda|\cos\theta| - \Delta\varphi_{nat}sgn(\cos\theta) \tag{1.11}$$

As required, the total membrane potential in the absence of $E_{\text{ind}}$, but viewed in the direction of the external field vector $E$, is given by $\Delta\varphi_m = \Delta\varphi_{\text{nat}}sgn(\cos\theta)$.

The geometrical amplification factor $a/d_m$ of a larger spherical shell, for instance, radius $a = 5$ µm and $d_m = 5$ nm is as large as $a/d_m = 10^3$. It is this geometrical amplification which rationalizes that comparatively small external fields in the range of $E = 1$ kV/cm are amplified to yield the large field strength $E_m = 10^3$ kV/cm, which then has such high (electroporative) power on the membrane structure.

### 1.1.8 Positional Averages

It is recalled that the membrane potentials, which are induced by the external field, are position dependent. For proper data analysis, it is instrumental to realize that the respective experimental electroporation parameters of homogeneous cell suspensions reflect the angular average of the different local poration reactivities (pore densities) at the polar angle $\theta$.

The overall membrane field $E_m$ induced by the applied field E can be expressed in terms of the positional average $\langle |\cos\theta| \rangle$. Since the field is poratively active as $E^2$, the effective field strength is

$$E_m = \langle E_m^2(\theta) \rangle^{1/2} = (E_m^2(0) \langle |\cos^2\theta| \rangle)^{1/2} = g(a/d_m) E f_\lambda (\langle |\cos^2\theta| \rangle)^{1/2} \tag{1.12}$$

Note, for charged surfaces and pulses of duration larger than $\mu$s or low frequency a.c. pulses, the g factor has to be calculated from the Dukhin factor with the respective medium conductivity. For ultra-short pulses or high frequency a.c. pulses, the geometric factor is $g = 3/2$.

On the same line, the distribution constant $K_p\,(E_m)$ is given by $\langle K(\theta) \rangle$. Therefore, analogous to the expression in Eq. (1.7), the average distribution constant is expressed $\langle K(\theta) \rangle$ as

$$\langle K(\theta) \rangle / K_0 = \exp\left[ b \left\langle \cos^2\theta(E_m) \right\rangle E^2 f_\lambda^2 \right] \tag{1.13}$$

The quantity b is given by

$$b = \frac{\langle \Delta\alpha_{pp} \rangle}{2k_B T} g^2 (a/d_m)^2 \tag{1.14}$$

The function $\langle \cos^2\theta(E_m) \rangle$ represents the field-dependent reactivity average and is limited to the range $1/3 \leq \left\langle \cos^2\theta(E_m) \right\rangle \leq 1$ for $E = 0$ and the virtual "E-infinity," respectively.

Comparing Eq. (1.7) with Eq. (1.13), the experimental quantity $K_p\,(E)$ is explicitly given as

$$K_p(E) = K_0 \exp\left[ b \left\langle \cos^2\theta \left( E^2 f_\lambda^2 \right) \right\rangle \right] \tag{1.15}$$

It is recalled that $K_0$ contains the "zero-field" standard value of $\Delta_r G^0$ containing the sum of the chemical structural contribution of pore fluctuations, the interfacial parameters of pore line tension, and membrane surface tension, membrane curvature, and bending rigidity [9].

Using $f_p(E) = \langle f_p(\theta) \rangle$, the experimental pore density fraction $f_p\,(E)$ is, in line with Eq. (1.4), specified as the polar angle average quantity:

$$f_p(E) = \frac{K_p(E)}{1 + K_p(E)} = \frac{K_0 \exp[b\langle \cos^2\theta(E_m)\rangle E^2 f_\lambda^2]}{1 + K_0 \exp[b\langle \cos^2\theta(E_m)\rangle E^2 f_\lambda^2]} \tag{1.16}$$

At the half-point of the fractional electroporation, we have $f_p = 0.5$; the respective half-point field strength is $E_{0.5}$. Because at $f_p = 0.5$, the half-point value of $K_p$ is $K_p(E_{0.5}) = 1$. For this case, we have in logarithmic form $\ell n K_0 = -b\langle \cos^2\theta(E_{0.5})\rangle E_{0.5}^2 f_\lambda^2$. As a practical estimate, we may use $\langle \cos^2\theta(E_{0.5})\rangle f_\lambda^2 = 1/2$, including $f_\lambda = 1$. Hence $K_0 = \exp\left[-(b/2)\cdot E_{0.5}^2\right]$ may be estimated and, later in the analysis, subjected to iterative refinement.

### 1.1.9 Experimental Data Correlations

If the measured quantity *Sig* $(E)$, e.g., signal due to uptake of a dye or of DNA or RNA, can be judged to reflect proportionality to the (pore) fraction $f_p$ $(E)$, see Eq. (1.3), the practical approximation is defined as

$$f_p(E) = Sig(E)/Sig(\max) = [P(E)]/[P]_{\max} \tag{1.17}$$

Indeed, the majority of measured field dependencies of *Sig* $(E)$ look as if they reflect Eq. (1.16), starting sigmoid exponentially and continuing toward saturation. Due to the usually very low value of $K_0$, the experimental data correlation *Sig* $(E)$ appears as an "onset $E^2$ scale-shifted" exponential. This characteristic feature deceives a "threshold field strength" $E_{\text{th}}$, operationally denoted as the field strength range where the Sig $(E_{\text{th}})$ becomes "visible" under the given experimental conditions. In single-pulse experiments, the value of $E_{\text{th}}$ is dependent on the pulse length (and the observation time).

It is noted that, at the start of the data analysis, the term *Sig* (max) is at first a virtual quantity similar to P(max) and later accessible by iterative fitting.

In any case, the evaluation of the characteristic system parameters from the experimental data is rather involved and has to proceed in several steps. The first step is to explore the so-called "low-field strength range" of the data correlation *Sig* $(E)$ as a function of the applied field strength $E$ by using the small-field approximations ${f_\lambda}^2 = 1$ and $\langle \cos^2\theta(E)\rangle = 1/3$. Recalling Eq. (1.15) and using Eq. (1.17), the initial part (up to about $f_p = 0.2$) of the experimental data correlations *Sig* $(E)$ can be analyzed in the explicit form:

$$K_p(E) = K_0 \exp\left[b' E^2\right] = Sig(E)/Sig(\max) \tag{1.18}$$

Practically, the low-field data are evaluated according to

$$\ell n|Sig(E)| = \ell n|Sig(\max)K_0| + b'E^2 \tag{1.19}$$

The slope yields the (experimental) term $b' = (1/3)\ b$ and the intercept (at $E = 0$) is $\ell n|Sig(\max)K_0|$. The term $Sig(\max)$ can be determined from the product $Sig(\max)$ $K_0$ if an estimate of $K_0$ is used. The value of $K_0$ may be estimated in two ways. The sigmoidal data function Sig (E) allows the estimation of a turning point range at the half-point field strength $E(\text{at } f_p = 0.5) = E_{0.5}$ by using the maximum of the derivative $d/Sig(E)|/dE$. If we now apply the slope value $b'$, $K_0$ is estimated from the relationship $\ell n\ K_0 = -(b/2)\ E_{0.5}^2$, using the estimate $\langle \cos^2\theta(E_m)\rangle = 1/2$ as a mean value for this initial range of the field strength. Since $Sig(\max) = 2\ Sig(E_{0.5})$, $K_0$ can also be estimated from the intercept $\ell n|Sig(\max)K_0|$ by inserting a rough visual estimate of $Sig(\max)$.

In the next step, the entire "zero-membrane conductivity transition curve," i.e., for the case $f_\lambda^2 = 1$, is calculated according to $f_p(E) = K_p(E)/\big(1 + K_p(E)\big)$ using the estimates for $K_0$, the slope value $b$, and the exact function $\langle \cos^2\theta(E_m)\rangle$ in the limits of 1/3 and 1. The differences between this curve and the actual data points yield the conductivity factor as a function of the applied field strength. From the value of $\langle \Delta\alpha_{pp}\rangle$, eventual pore polarization volume and pore radius may be calculated.

### *1.1.10 Flux Coefficient Integrals*

The newly introduced concept of time-dependent flux coefficient functions has turned out to be instrumental for proper flux analysis [16] of the post-field conductance relaxations (resealing curves) reflecting transport through a decreasing number of pores. It is practical to start the analysis of the measured signals, for instance, conductance relaxations $g$(t) with the introduction of reduced signals like signal ratios $Y$(t). For example, the time course of the signal ratio $Y(t) = (g(t) - g(0))/g(0)$ $= (I(t) - I(0))/I(0)$ of the after-field currents ($I$) or conductances ($g$), relative to the zero time values $I(0)$ and $g(0)$ before pulse application, looks like an increasing "stretched exponential" of the Kohlrausch type. However, the nonequilibrium concept of a flux coefficient function $k$(t) provides an expression in terms of an "exponential of an exponential." Explicit, instead of the simple exponent term $kt$, where $k$ is a constant flux coefficient, the exponent term in the respective $Y(t)$-function is an integral $\int k(t)dt$, such that $Y(t) = Y(\max)\ \exp[-\int k(t)dt]$. For instance, if in the simplest case of monoexponential pore resealing during the efflux phase, the efflux coefficient function is given by, $k_R(t) = k_0(t_p, E)\exp[-t/\tau_R]$, where $k_0(t_p, E)$ is the initial value of the flux coefficient at the end of the pulse (at $t_p$ and $E$) and $\tau_R$ is the ensemble time constant for pore resealing. Note, at this time point the new time scale starts at $t = 0$ for the post-field efflux function $Y(t)$. The integral is given by

$$\int k_R(t)dt = k_0(t_p, E)\tau_R[1 - \exp(-t/\tau_R)]\} \tag{1.20}$$

Insertion of Eq. (1.20) yields the integral function [7, 9]:

$$Y(t) = Y(\max)\{1 - \exp\{-k_0(t_p, E)\tau_R[1 - \exp(-t/\tau_R)]\}\} \tag{1.21}$$

In Eq. (1.21), $Y(\max)$ refers to the virtual maximum value for the case of complete equilibration between the intracellular ion concentration and that of the external medium. The stationary value $Y(ss) = Y(t \to \infty) \leq Y(\max)$ may be estimated by extrapolation (parallel to the abscissa). It refers to the stationary value of resealing (before concentration equilibration) and is given by

$$Y(ss) = Y(\max)\left(1 - \exp\left[-k_0\left(t_p(E)\tau_R\right)\right]\right) \tag{1.22}$$

In terms of pore fraction, the ensemble resealing of the porous area in the absence of the field is given by $f_p(t) = f_p(E)\exp[-t/\tau_R]$.

This procedure of analysis was, for instance, successfully applied for the resealing phase of densely packed CHO cells. As rationalized with Eq. (1.21), the measured transport curves are therefore exponentials of exponentials. The actually measured curves can deceive stretched exponentials (of the Kohlrausch type). As seen in the case of exponential decrease in the pore fraction, the post-field kinetics provides mechanistic details of the long-lived electroporated membrane states. This analytical framework has been used to obtain the values of $k_0$ $(E, t_E)$ as a function of the field strength E and of the pulse duration $t_E$, respectively, and of the (field-independent) time constant $\tau_R$ of the resealing process [7].

Complementary to efflux of ions into the outer cell compartment, influx of a dye into a cell, for instance, is analyzed in a similar way [11]. If the measured signals $Sig(t)$ can be expressed as the fraction $y(t) = Sig(t)/Sig(ss)$, where the stationary signal is given by the amplitude, $Sig(ss) = S(t \to \infty)$. The proper differential equation describing the signal increase is formally analogous to the linear form of $dy(t)/d(t)$:

$$\frac{d\,y(t)}{dt} = -k_p(t)[y(t) - y(ss)] \tag{1.23}$$

where $k_p(t)$ is the influx coefficient function and the stationary term, $y(ss) = Sig(t \to \infty)/Sig(ss) = 1$. Integration of Eq. (1.23) yields the integral flux equation for the stretched increasing (or the delayed increasing) time course:

$$y(t) = y(ss)\left(1 - \int k_p(t)dt\right) \tag{1.24}$$

In the linear case, the flux coefficients for the (apparently stretched) increase are $k_p(t) = k_0\exp[-t/\tau_p]$ and, for the delayed increase, $k_p(t) = k(ss)\exp[1 - t/\tau_p]$, respectively.

### 1.1.11 Elementary Kinetics of Electroporation

Since pore formation is a chemical structural process involving lipid reorganizations and interfacial water molecules, see Eq. (1.1), the kinetic analysis uses "chemical" rate equations. In terms of the scheme in Eq. (1.2), the individual rate equation for a particular relaxation mode of the increase in the pore density is given by

$$\frac{d[P(t)]}{dt} = -k_p(t)[P(t) - P(ss)] \tag{1.25}$$

In Eq. (1.24), *P(ss)* is the conventional relaxation amplitude and the term, $k_p(t)$ represents the reaction flux coefficient function. It replaces the normal relaxation rate term $1/\tau_p = k_p + k_{-p}$, where *kp* is the ensemble poration rate coefficient and *k-p* is the pore closing ensemble rate coefficient. In the case of a sigmoid onset of the integral relaxation curve, we may use the membrane conditioning coefficient (dimple formation preceding the actual pore formation process) in the form of $k_p(t) = k(ss)\exp[1 - t/\tau_{cond}]$.

Here, *k(ss)* is the constant stationary coefficient and $\tau_{cond}$ the ensemble time constant of the respective conditioning process. We may start with the assumption of proportionality between the measured quantity Sig(t) and [P(t)]. Consequently the integrated rate equation is given by

$$Sig(t) = Sig(max)\{1 - \exp[-k(ss)(t - \tau_{cond}(1 - \exp[-t/\tau_{cond}])\Big)]\} \tag{1.26}$$

In Eq. (1.26), the—at first—virtual term *Sig*(max) is given by the measured stationary value

$$Sig(ss) = Sig(max)\Big(1 - \exp[-k(ss)\tau_{cond}]\Big) \tag{1.27}$$

Analogous to $K_p$, the field dependence of the rate coefficient is given by the Arrhenius-like equation: $k(E) = k(0)\exp[-G^*(E)/RT]$, respectively, for the on-rate coefficient and the off-rate coefficient, where $G^*(E)$ is the respective field-dependent Gibbs activation free energy [12].

In each case, however, it must be checked which equation must be applied and whether existing equations have to be modified or expanded [12], as dictated by proper physical chemical reasoning along the fundamental laws of flux nonequilibrium thermodynamics.

## 1.2 Millisecond and Microsecond Pulse Effects: An Introduction

Richard Heller, P. Thomas Vernier, and Justin Teissie

Electric fields can be used to elicit specific responses from biological cells. Research exploring these effects has been ongoing since the 1960s [17–22]. The electric fields are typically applied as a series of short-duration pulses and are easily obtained by applying a voltage pulse between a set of two conducting electrodes in contact with the sample. The time course and the magnitude of the field are directly controlled by the voltage generator and the electrode geometry. The voltage is obtained by charging a capacitor that is discharged under the control of a trigger in an electronic circuit that controls the decay. This can be an exponential decay or a square pulse of a controlled duration. Pulse duration (or decay) is from micro- to milliseconds (see details in Chap. 2). The specific effect on the cell(s) exposed to the field is dependent on the pulse characteristics (amplitude, duration, and number). With micro-millisecond pulse durations, the effect is predominately on the cell membrane and can result in reversible or irreversible permeabilization. Reversible permeabilization also known as electroporation and electrotransfer can be used to move molecules from one side of the membrane to the other, including large molecules such as proteins and nucleic acids. When pulse characteristics are chosen, appropriately cells will typically survive the reversible permeabilization process. Irreversible permeabilization (electroporation) is done to induce cell death. This approach can be used to effectively ablate tissue such as solid tumors without causing damage to vital structures. Another result of the application of pulse electric field is fusion between two cells that are in contact when the field is applied.

### *1.2.1 History*

There is evidence through scientific history of the use of electric fields in biomedical applications. This includes evidence from the first century that Largus utilized electric fields as a treatment for taste and headaches [23]. In the eighteenth century, several scientists utilized electric fields to evaluate the effects on animals, human skin, muscle contractions, and basic responses of humans following electrical stimulation [24–28]. In the twentieth century, work is more focused on the effects on cells and the potential uses of these fields. In 1959, Pauly and Schwan reported on an electrophysical model of a cell [29]. Coster reported on the ability to use electricity to punch through biological membranes [17], and Hamilton and Sale demonstrated how electric pulses could cause damage to cell membranes [30].

Following these breakthroughs in the 1960s, work began to evaluate utilizing electric fields to manipulate cells and cell membranes. In the 1970s several

breakthroughs occurred. The work during this decade focused on the membrane effects following brief exposure to intense electric fields. Neumann and Rosenheck in 1972 reported on permeabilization of vesicular membranes [3]. In 1974, Zimmermann et al. reported on increasing membrane conductance [22]. In the late 1970s, focus shifted more toward membrane breakdown and how this could be utilized. Kinosita and Tsong demonstrated the electroporation of erythrocytes in 1977 [31]. Electrical stimulation and fusion of plant protoplasts were accomplished in 1979 by Senda et al. [32]. This was followed in 1981 with Scheurich and Zimmermann successfully fusing different plant protoplasts [33]. Transient electroporation in phospholipid vesicles was demonstrated by Teissie and Tsong in 1981 [34]. Gordon and Seglen demonstrated reversible permeabilization to accomplish small-molecule uptake in 1982 [35]. In that same year, Neumann et al. demonstrated that genes could be delivered to mammalian cells using electric pulses [1]. Also in 1982, Teissie et al. demonstrated electrofusion of fibroblasts [36]. Potter reported on a standard method for in vitro gene electrotransfer in 1984 [37]. Sugar, Neumann, and Chizmadzhev reported on a model of aqueous pore in the late 1970s early 1980s [13, 38]. The work performed in the 1970s and 1980s formed the foundation for the current description of both electroporation and electrofusion. In addition, the studies performed during this era made critical contributions to the basic description of the interaction between electric pulses and biological membranes. This confirmed that intense electric fields could be used to destabilize membranes to facilitate transport and that this effect could be reversible, preserving the cell viability.

In the late 1980s, the focus shifted to utilizing electric fields for specific applications. Electrofusion was utilized to facilitate the production of monoclonal antibodies [39]. In 1986, Okino and Mohri reported on using pulse electric fields to deliver chemotherapeutic agent (bleomycin) to a tumor in a mouse model [40]. Mir et al. optimized this approach demonstrating the potential as an anticancer therapy [41]. This approach was later expanded to include other chemotherapeutic agents, calcium delivery, electrode devices, and administration routes [42–44]. This work was translated into clinical use with the first clinical results being reported by Mir et al. in 1991 [45]. The in vivo delivery of genes was first reported in 1991 by Titomirov purpose; while the delivery was done in vivo, the expansion and detection were done in vitro [46]. The first complete in vivo delivery of plasmid DNA was accomplished in 1996 by Heller et al. [47]. The first delivery to a solid tumor was accomplished in 1998 by Rols and Teissie [48] and to muscle by Aihara et al. [49] The delivery of DNA has also been translated to clinical use with the first clinical trial being reported in 2008 by Daud et al. [50] The use of pulse electric fields has also been used for transdermal delivery as demonstrated by Prausnitz and Weaver in 1993 [51, 52]. Electric fields can also be used to directly ablate tumors by performing irreversible electroporation. This was initially demonstrated by Davalos, Mir, and Rubinsky in 2005 [53]. In the late 1980s and early 1990s, Grasso et al. demonstrated that electric pulses could be used to fuse cells directly to tissue both in vitro and in vivo [54, 55].

### 1.2.2 Physical Effects on Membranes (Experiments and Modeling)

The first effect of applying a voltage pulse on a conducting sample is Joule heating. The temperature of the sample is increased. This affects the thermodynamic properties of the membrane. The amount of heating is dependent on the number of pulses and the time between pulses. The shorter the time between pulses, the more of an effect on heating [56].

The second effect is to induce electromechanical stress on the cells. The molecular organization of the membrane is altered. Charged species are submitted to an electrophoretic drift. The domain organization in the membrane is changed [57].

Cells can be considered as "spherical capacitors." The membrane is indeed a dielectric thin layer. The external field induces a charge loading of the membrane that is position dependent due to the vectorial character of an electric field. This charging time ranges from submicrosecond to a few microseconds. As a result, the transmembrane potential is heterogeneously modified during the application of the field pulse [58].

Details are in Sects. 4.1, 4.2, and 4.4.

### 1.2.3 Primary Biological Effects (Cytoplasmic Content Changes and Swelling)

The most dramatic consequence is the observation of a membrane alteration to a permeabilized state. Polar compounds that cannot freely cross the membrane under normal resting conditions are observed to freely diffuse across it after application of pulses with appropriate characteristics. This new organization can be reversible or irreversible [3].

Under reversible conditions, the cytoplasmic content is going to be changed. Due to the leakage, secondary messengers leave the cytoplasm. At the same time, new species will flow inside such as Ca2+. This results in a dramatic alteration of the cell organization. Organelles (nucleus) and cytoskeleton are the main targets of these changes. An additional change is that the cell undergoes osmotic swelling. Those primary biological effects are secondary consequences of the physical trigger (the electric field pulse). These changes are transient as the membrane is going to reseal and recover its characteristic-specific permeability. Through an active process (dependent on the energetic reserves of the cell), the cytoplasm will be brought back to normal [59–61].

Under irreversible conditions, the membrane cannot recover and cell death follows. When cells are aligned properly during the administration of pulses, fusion may occur. This will result in a multinucleated cell. Cells can survive this process [62].

Details are in Sects.. 4.4 and 4.9.

### 1.2.4 Secondary Biological Effects (Fusogenicity, Apoptosis, etc.)

Even when membrane permeabilization is reversible, the cytoplasmic alteration may result in a cascade of reactions involving the organelles. In these circumstances, it is possible that the cell will undergo apoptosis.

Membrane electropermeabilization is a complex multimolecular event affecting the interfacial properties of the cell surface. When cells are brought into contact during (or after) the electric pulse application, membrane merging between the two partners is observed as well as their content mixing. This is the direct evidence that membrane fusion is mediated by the electric pulse application.

Details are in Sects.. 4.4, 4.6, 4.7, and 4.9.

### 1.2.5 Medical Applications

A major application of administration of pulse electric fields is to deliver molecules with therapeutic or prophylactic potential to the interior of cells. Cell membrane is an important protective barrier for cells. However, the membrane can also be a barrier preventing therapeutic molecules from reaching their intracellular targets. In the case of chemotherapeutic agents, the influx or efflux of the drug can be influenced by the presence or absence of specific receptors or transport proteins that move the drug out of the cell. The use of pulse electric fields can bypass this process by giving the agent a more direct path into the cytosol. By allowing uploading of hydrophilic compounds to the cytoplasm, electric pulses give access to their cytoplasmic target to drugs that can only very poorly cross the plasma membrane spontaneously. In addition, delivery in this manner will typically result in higher concentrations of the drug within the cell thereby reducing the impact of transport proteins moving drug out of the cell. Lower drug concentrations can be used to obtain the clinical effect minimizing the secondary effects of chemotherapy. This approach has been named electrochemotherapy (ECT) and has been under development since the middle of the 1980s and is now a routine practice in Europe, where the equipment is approved by the regulatory agencies [63].

Delivery of nucleic acids is another major application of reversible permeabilization and its use has been steadily growing. Nucleic acids are significantly larger than drugs and cannot easily pass through the cell membrane. The administration of pulse electric field with the appropriate characteristics provides a means to move nucleic acid into the cell even within a tissue. Immune responses against the protein coded by the transferred plasmid can be induced resulting in efficient delivery of DNA vaccines. Another promising approach is to boost the immune expression by the expression of cytokines. Common target tissues are the skin, tumor, or muscle that are easily accessible for the electrodes and therefore for a calibrated field pulse delivery. The approach has been successfully translated

from laboratory and preclinical models to both human and veterinary applications [50, 64–68].

Membrane fusion can be used for the production of hybridomas for the production of monoclonal antibodies [39]. It can also be used to make phenotypical changes within cells.

Pulse electric fields can also be used to have direct effect on cells and tissues. Using pulse characteristics that result in irreversible permeabilization can result in death of exposed cells [52]. This can be used to ablate solid tumors. In this case, the pulse electric field directly causes the destruction of the tissue instead of using the fields to deliver the effector molecule. The irreversible approach can be done in a manner that does not significantly elevate temperature which reduces or eliminates effects on vital structures. This clinical technology is now on the market.

This is described in detail in Chap. 5.

### *1.2.6 Biotechnological Applications*

Membrane permeabilization through the use of pulse electric fields can be utilized to extract substances from cells. This can be utilized to enhance yields of products being collected from cells acting as "factories" for specific substances (yeast, microalgae, plants). This can be used to enhance olive oil production, lipid extraction, anthocyanin extraction from red cabbage, extraction of juice, or wine production. The technology has advanced to the point that electroextraction is now used at the industrial level through the development of flow process treating hundreds of liters per hour. A suspension of cells is pumped through a chamber, where electric pulses are delivered at high frequencies [69].

Irreversible permeabilization of bacteria and yeasts is now used in the food industry for cold sterilization preserving the taste of the electrotreated product. Here again flow processes are routinely used. A similar approach is under development to treat wastewater without the use of chemicals [70].

Gene engineering by electrotransfer is used routinely in applications for the obtention of GMO. A major advantage is that gene transfer is obtained on walled species (yeast, bacteria) not on protoplasts. This makes regeneration easier [71–74].

Membrane fusion between protoplasts can be used for the production of hybrid cells [75].

This is detailed in Chap. 6.

## 1.3 Nanosecond and Picosecond Pulse Effects: An Introduction

Karl H. Schoenbach and Stephen J. Beebe

### *1.3.1 From Classical Plasma Membrane Poration to Subcellular Membrane Effects*

The effect of intense pulsed electric fields on biological cells and tissues has been the topic of research since the late 1950s. Intense means that the electric field is of sufficient magnitude to cause instant, nonlinear changes in cell membranes. The first paper reporting the reversible breakdown of cell membranes when electric fields are applied was published in 1958 [76]. The first report on the increase in permeability of the plasma membrane of a biological cell, an effect subsequently named "electroporation," appeared in 1972 [3]. The electric fields that are required to achieve electroporation depend on the duration of the applied pulse. Typical pulses range from tens of milliseconds with amplitudes of several 100 V/cm to pulses of a few microseconds and several kV/cm.

More recently, the pulse duration range has been shortened into the nanosecond range. The effects of such short pulses have been shown to reach into the cell interior [77]. Pulse durations are as brief as several nanoseconds, with pulse amplitudes as high as 300 kV/cm for short pulses [78]. A new field of research opens when the pulse duration is decreased even further, into the subnanosecond range. By applying such ultrashort pulses, it will also become possible to use wideband antennas, rather than direct-contact electrodes, to deliver the pulses to tissue [79].

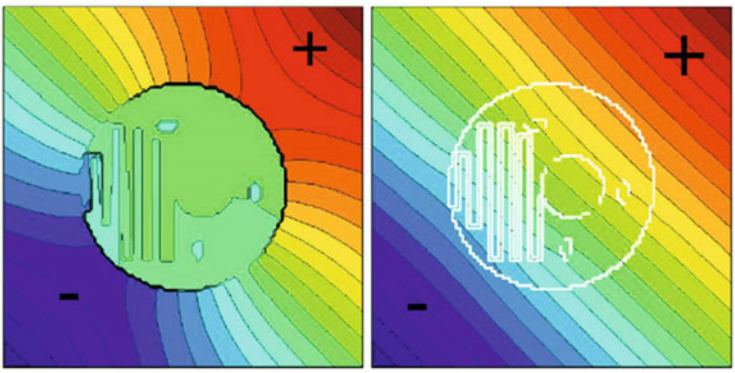


**Fig. 1.2** The effect of 7 μs long pulses with 1.1 kV/cm field amplitude (*left*) and that with 60 ns at 60 kV/cm amplitude (*right*) on cells. The electrical parameters were chosen such that the electrical energy for both cases is identical [85], with permission

The prediction that ultrashort pulses cause intracellular effects was based on a simple analytical, passive, and linear electrical model of the cell. In this model, the cell membranes, plasma membrane and subcellular membranes, were considered as capacitors and the cytosol and the medium inside the organelles as resistors [77, 80]. Passive and linear mean that changes in the properties of the cell structures, such as electroporation, are not considered. The assumption holds strictly, therefore, only for electric field amplitudes below those required for electroporation or nanoporation. The results of this model indicated that for pulses on the order of or less than the charging time constant of the plasma cell membrane, $\tau_m$, the applied electric field reaches into the interior of the cell and therefore affects cell substructures and possibly cell functions. Since typical charging time constants of cells with dimensions of 10 μm are on the order of hundred nanoseconds, submicrosecond pulses were expected to cause different effects on cells than pulses with durations of microseconds and longer.

After the onset of poration, this simple linear, passive element approach is no longer applicable to describe electric field–cell interactions. The membrane becomes then an "active" cell element, with variable resistivity and variable permeability. Modeling of cells with "active" membranes had been a topic of multiple publications [81–84]. A detailed discussion on modeling by J. Weaver can be found in Sect. 4.2. Figure 1.2 shows the results of a continuum model [85, 86]. Here, the poration of the plasma membrane and subcellular membranes was compared for pulses of 7-μs and 60-ns duration. The electric field of the pulses was adjusted such that the energy density in both cases was identical. For 60-ns long pulses, (left) the cell membranes, plasma and internal, are fully exposed to the applied 60-kV/cm pulse, clearly demonstrating that nanosecond pulses allow us to affect subcellular membrane potentials. When the cell was exposed to a long pulse (7 μs) at 1.1 kV/cm, effects were only seen on the plasma membrane. The cell interior is shielded.

Under the conditions mentioned above (assuming that all membranes are equal, and the conductivity of organelle interiors and cytosol is the same), the voltage across the organelle membranes never exceeds the voltage across the plasma membrane. However, if we deviate from these assumptions and take into account that cell and organelle membranes differ electrically as do their interiors, it is possible to construct scenarios where the voltage across the organelle membranes exceeds that of the plasma membrane in a certain spectral range. This has been shown by using a simple equivalent circuit but assuming a lower capacitance of subcellular membranes (thicker membranes) than that of the plasma membrane [77, 87]. Similar results have been reported using a more elaborate continuum model, by Kotnik and Miklavcic [88]. Also, a cell membrane of low curvature requires a larger voltage to be electroporated than a highly curved membrane of small vesicles [89]. Consequently, under certain conditions, poration of subcellular membranes could be more likely than plasma membrane poration.

The first experimental study on the effect of nanosecond pulses on the intracellular structures showed that such pulses affect membranes of subcellular structures [77]. Human eosinophils were loaded with calcein-AM (calcein-

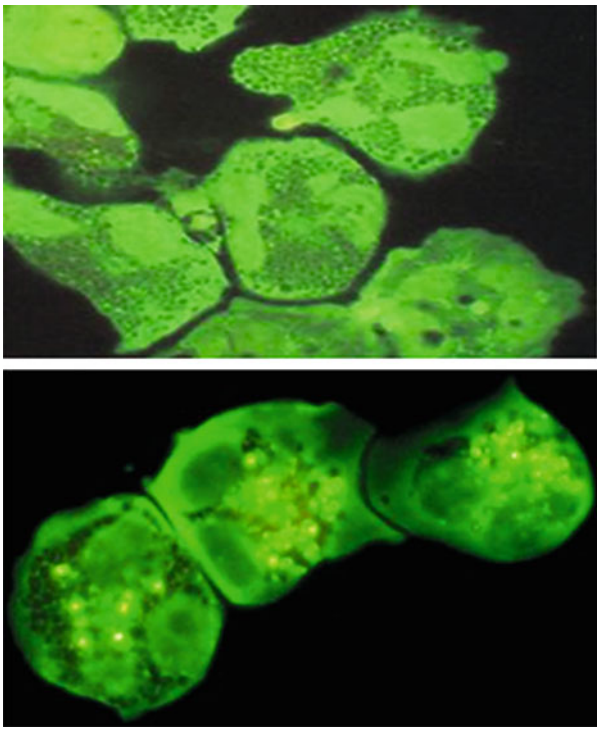

**Fig. 1.3** Eosinophils (white blood cells) before (*top*) and after (*bottom*) the application of 60 ns pulses with electric fields of 50 kV/cm—photograph on bottom shows that inner structures have opened and taken up dyes—shown as "sparklers" [77] © [2001] John Wiley & Sons, Inc

acetoxymethylester), an anionic fluorochrome that enters cells freely and becomes trapped in the cytoplasm by an intact cell surface membrane following removal of the AM group. The granules in the eosinophils stay unlabeled because the cytosolic calcein is impermeant to the granular membrane. When 60-ns long pulses with an electric field amplitude of 50 kV/cm and higher were applied to the eosinophils suspended in Hanks Balanced Salt Solution, the granules, which were dark (nonfluorescent) before pulsing, began to fluoresce brightly (Fig. 1.3). This is a strong evidence for the breaching of the granule membranes and ionic binding of free calcein from the cytosol to the cationic granule components. On the other hand, the retention of the cytoplasmic calcein staining indicated that the surface (outer membrane) was not electroporated in such a way that it became permeable for these ions.

#### 1.3.1.1 Nanoporation of Membranes

There is definitely an effect of nanosecond pulsed electric fields (nsPEFs) on the plasma membrane. Laser stroboscopy with a temporal resolution of 5 ns showed a rapid increase in membrane conductance in only a few nanoseconds when a 60-ns, 100-kV/cm pulse was applied [90]. The increase is assumed to be due to the

formation of nanopores. This concept of nanoporation, the creation of a high density of "nanopores," had been introduced by Joshi [81] and by Weaver [86, 91]. These are pores of such small diameters (1.5 nm) that they become permeable only for small ions. Using whole-cell patch clamp to measure plasma membrane conductance changes resulting from nanosecond pulsed electric field (nsPEF) exposure, such nanopores have been observed following nsPEF exposure [92]. In Sect. 4.5 by A. Pakhomov, nanoporation is discussed in more detail. Molecular dynamics simulation is a method which is particularly suitable to study these nanopores. The importance of this method is in the visualization of membrane effects on timescale of nanoseconds, the inclusion of complex underlying physics, and the determination of critical electric fields for pore formation [93–96]. T. Vernier provides an overview on "molecular dynamics in electropermeabilization" in Sect. 4.3.

#### 1.3.1.2 Scaling of Nanosecond Pulse Effects

Studies in the nanosecond and even in the near subnanosecond (700 ps) range indicate that nanosecond bioelectric effects, $S$, scale with the product of electric field, E, times pulse duration, $\tau$, times the square root of the number of pulses, $N: S = S\left(E\tau N^{1/2}\right)$ [97]. Such a scaling law can be understood by assuming that the intensity of the bioelectric effect is proportional to the total number of ions passing through the cell membrane or, in other words, depends primarily on the current density (times the pulse duration). The square root dependence on the pulse number in in vitro studies can be considered the result of the thermally initiated statistical rotation of cells with respect to the electric field direction. It needs to be noted that this scaling law for nanosecond pulses has been derived for monopolar pulses. For pulses of different shape, it will need to be modified. Recent measurements of the diminished calcium uptake of cells when bipolar pulses are applied [98] could possibly be explained by drift as the major transport process for the ions through the nanoporated plasma membrane. The "reverse drift" model for bipolar pulses indicates a reduced importance of diffusion for nanosecond pulses and allows estimates on the recovery time of membranes [99].

### *1.3.2 Biological Effects*

Whereas the previous section introduced biophysical effects of nanosecond pulses, especially effects on plasma membranes, the following will give a brief overview on biological studies of nanosecond pulsed electric fields: intracellular signaling, physiological functions, and apoptosis or regulated cell death (RCD) induction. In early experiments (1997–2005), new biological applications for nanosecond pulse power technology, which had been used for decades mainly for military purposes,

were realized. This was of much interest because organisms had not evolved to respond to such brief and intense electric fields, which did not exist in nature. Thus, cells must use mechanisms that evolved for responses to other stimuli, most likely other stresses, especially when electric field intensities are high. (This aspect will be presented in a chapter devoted to biological responses.) In addition, given that nsPEFs had been shown to kill bacteria [100, 101], it seemed to be possible that this technology has application for cancer therapy. Therefore, mechanisms for cell death induction were of specific interest.

A variety of effects in living systems both in vitro and in vivo have been observed in response to nsPEFs depending on the pulse duration, electric field amplitude, and the number of pulses. With pulse repetition rates of one to two pulses per second, elevated temperatures could be circumvented, and responses were strictly due to nonthermal, electric fields. Since submicrosecond pulses were hypothesized to induce intracellular effects [77], early analyses were focused on effects on intracellular membrane permeability, calcium mobilization, and typical responses indicative of apoptosis, including phosphatidylserine externalization, caspase activation, cytochrome *c* release, and/or DNA damage as well as cell viability. These early studies revealed a number of fundamental observations about how cells responded to nsPEFs.

As might be expected, longer pulses with higher electric fields were found to be more effective for all cell responses than shorter pulses with lower electric fields, and essentially all cell responses were electric field and pulse number dependent. As pulse durations were shortened, higher electric fields were required for given effects seen at longer pulse durations. Furthermore, for many nsPEF effects, including ethidium homodimer uptake (HL60, Jurkat), phosphatidylserine externalization (Jurkat), caspase activation (HL60, Jurkat), and cytochrome *c* release (Jurkat), numbers of "sparkler" granules per cell and viability for human eosinophils did not scale with energy density, which is consistent with nonthermal responses. In general, for cell death and apoptosis induction, longer pulses and/or higher electric fields were required, while reversible effects on plasma membranes and calcium mobilization could be observed at lower electric fields. These fundamentals will be reiterated in the sections below.

#### 1.3.2.1 Calcium Mobilization and Intracellular Calcium Release

Most of the research in the lower range of pulse amplitudes was focused on its effect on the release of intracellular free calcium. Calcium is known as a ubiquitous second messenger molecule that regulates a number of responses in cell signaling, including modulation of metabolism, gene transcription, secretion of neurotransmitter and hormone, muscle contraction, and proliferation and apoptosis regulation, among others. Intracellular calcium is primarily stored in the endoplasmic reticulum (ER) (α-granules in platelets) with lower levels in mitochondria. Nevertheless, several mitochondrial enzymes are calcium dependent, and there is continuous

calcium cycling between the two organelles. Calcium is not only important for life, but calcium-overloaded mitochondria are a harbinger for cell death [102, 103].

One of the earliest demonstrations of submicrosecond pulses on calcium mobilization was carried out with human polymorphonuclear leukocytes (PMNs). When the PMNs, crawling over a coverslip between electrodes, were exposed to a 300-ns pulse with an electric field strength of 15 kV/cm, apparent random fluctuations in intracellular calcium levels abruptly changed to cellular coordinated spikes in intracellular calcium with cessation of crawling followed by slowly decreasing levels in intracellular calcium when cells become mobile again 7–10 min after the pulse [104]. The immobilization phase was electric field dependent. Lowering the electric field allowed cells to recover mobility and fluctuations in intracellular calcium more quickly. This mobility effect had been previously observed when aquatic organisms, such as brine shrimp [61] or hydrozoans [105], were subjected to submicrosecond pulsed electric fields; however, this was the first demonstration of reversible coordinate effects on calcium dynamics and cell function.

The origin of this calcium release was not determined, but was later shown in other cell types to be from extracellular sources through permeabilized plasma membranes as well as from intracellular sources such as the endoplasmic reticulum (ER). In experiments where cells were treated with nsPEF in the absence of extracellular calcium, elevation of intracellular calcium was observed coming from intracellular stores [104–109]. One reason for the observed calcium emission from intracellular stores was the nanoporation of the subcellular membranes, in line with the initial assumption that the high electric fields generated by the nanosecond pulses cause permeabilization of these membranes. Another explanation for how nsPEFs induce calcium release from the ER is that the nsPEFs mimic a ligand signal that triggers receptors on internal membranes, thus causing calcium to be released from the internal stores into the cytoplasm [109].

NsPEFs also cause platelet calcium release and aggregation in human platelet-rich plasma and washed platelets [110], an effect which is now successfully used in wound healing. Activation and aggregation of platelets with nsPEFs will avoid adverse effects of adding exogenous thrombin for wound healing. This topic will be presented in greater detail in Sect. 5.5 by S. Beebe and B. Hargrave.

#### 1.3.2.2 Regulated/Programmed Cell Death

During development and homeostasis, cells that are no longer necessary, worn out, or damaged during cell division are eliminated by a programmed cell death (PCD) mechanism called apoptosis that is carried out by a genetically regulated program (s). The term “programmed” in PCD is specifically used to define a regulated cell death (RCD) that is part of a developmental program or used to preserve physiological homeostasis. In contrast RCD, while genetically programmed, can be “influenced,” at least partially, by specific pharmacologic or genetic interventions [111] and as it turns out “influenced” by electrical interventions [112, 113]. These developmental and homeostatic programs are initiated by extrinsic mechanisms

activated by cell death receptors on plasma membranes (extrinsic apoptosis) or by intrinsic mechanisms activated by internal signals in response to intracellular errors, stress, or defects (intrinsic apoptosis). Under these circumstances apoptotic cell death is anti-inflammatory and immunologically silent, protecting the organism from inflammatory and autoimmune complications. In vivo apoptosis was not readily observed under normal physiological circumstances even though millions of cells are dying by the minute. This is because apoptotic cells are phagocytized before their plasma membranes break and intracellular products that induce inflammatory reactions are contained and inhibited. Thus, the final stages of apoptosis take place inside phagocytes in these homeostatic occurrences.

This apoptotic process is different than necrosis, which has, until recently, been classically characterized as accidental cell death due to catastrophic, abrupt, and irreversible membrane permeabilization and characterized by inflammation and immunogenic recognition. Necrosis is now known to be programmed under certain circumstances and classified as programmed necrosis, one of several regulated cell death (RCD) mechanisms. While defects in apoptosis were first known to cause diseases, regulated necrosis is now known to play roles in physiological (embryonic development) and pathological (ischemic conditions) scenarios [111]. A later chapter is dedicated to mechanisms of RCD including apoptosis. However, at the beginning of experimentation with nsPEFs, around 1998, apoptosis was the only known mechanism of RCD (necrosis was not known to be programmed), and studies were focused to determine if nsPEFs induced apoptosis as a means for causing losses in cell viability.

Early experiments to investigate cell death were carried out with HL-60 cells and Jurkat cells for in vitro studies and fibrosarcoma tumors for ex vivo and in vivo studies using pulse-forming networks with coaxial cable or a strip line giving pulse durations of 10, 60, or 300 ns with electric fields as high as 280 kV/cm (28.0 MV/m) [108, 112, 113]. Another study was carried out in Jurkat and rat glioma cells using a MOSFET-based, inductive-adder pulse generator with pulse durations of 10 ns and electric fields of 28 or 40 kV/cm (2.8 or 4.0 MV/m) [114]. Generally, these studies showed that apoptosis was induced by ultrashort pulses when the electric field amplitude exceeded a threshold value. All of these studies showed differences in plasma membrane behavior between nsPEFs and classical electroporation pulses and used phosphatidylserine (PS) externalization and caspase activation as apoptosis markers.

These early studies on cell death induction demonstrated several fundamental aspect of how cells responded to nsPEFs, stimuli that were not present during evolution of the species. As might be expected, some cells were less sensitive to nsPEFs. For example, unlike the Jurkat cells, rat glioma C6 cells [75] and 3 T3–L1 pre-adipocytes [113], which normally grow attached to surfaces, were found to be highly resistant to the same pulses and pulse sequences. In other experiments where cell survival was explored after ultrashort pulse application, adherent cells required higher electric fields than nonadherent cells for cell death induction [115]. Generally, rapid progression of apoptosis induced by nsPEFs was quite different from that obtained with other apoptotic stimuli, such as UV light and toxic chemicals, which

require hours for apoptosis markers to appear. However, the kinetics of ultrashort pulse-induced apoptosis depends on the pulse duration. Shorter pulses result in slower apoptosis progression than longer pulses for the same electrical energy density [113]. Likewise, it is possible for shorter pulse durations to induce apoptosis by increasing electric fields or pulse numbers. For pulse regimens with higher pulse numbers, no systematic studies have been conducted to determine the effect of pulse repetition rate. However, these early studies, like many of later ones, used pulse conditions with relatively low repetition rates so that the electric field was the primary determinant or the only variable, because high repletion rates resulted in increases in temperature.

Since the initial discovery that nsPEFs trigger an apoptosis signaling pathway, there have been significant efforts made to determine the exact mechanism of this process. One of the possible reasons for nsPEF-induced apoptosis was suggested to be extensive intracellular calcium elevation [116]. Calcium at high concentration is known to induce apoptosis [116]. Another possible mechanism for apoptosis induction with ultrashort electric pulses was suggested by Weaver [2003]. The electric field of nanosecond pulses correlated to the high current density in the cytoplasm will affect subcellular membranes, e.g., mitochondrial membranes. It is known that biochemically induced apoptosis involves the mitochondrial permeability transition pore (mPTP) complex [113] and the mitochondrial membrane voltage-dependent anion channels [117, 118]. A hypothesis is that ultrashort pulses change the transmembrane voltage at mitochondrial membrane sites, which leads to an opening of the mPTP, inducing apoptosis [119].

More recent nsPEF studies experimentally demonstrate the importance of influxes of extracellular calcium and dissipation of the mitochondria membrane potential ($\Delta\Psi m$) for cell death [120–122]. However, calcium was necessary, but not sufficient to induce cell death; cell death was coincident with a decrease in the mitochondrial membrane potential, $\Delta\Psi m$, in a calcium-dependent manner. The calcium dependence for dissipation of $\Delta\Psi m$ is not consistent with a permeabilization event of the inner mitochondrial membrane, but is consistent with nsPEF-induced changes in the transmembrane voltage at mitochondrial membrane sites in the presence of elevated calcium, which leads to the opening of the mPTP and apoptotic cell death. This is a significant deviation from what is expected for nsPEF effects on intracellular membranes such as that observed for calcium release from the ER. Additional studies of nsPEF effects on mitochondria and $\Delta\Psi m$ will be necessary to further analyze this hypothesis.

More recently, a determining role for calcium in cell death was observed using HeLa cells [123]. Calcium was shown to not only be important for cell death but to determine what cell death mechanisms were activated in some cells. While non-apoptotic mechanisms of nsPEF-induced cell death were known [124, 125], no specific mechanisms were defined. However, in HeLa cells, calcium was shown to be required for a type of regulated necrosis identified by formation of poly (ADP-ribose) or PAR. While these cells could express apoptosis markers (caspase activation), they underwent PAR-associated regulated cell necrosis, which was suggested to be a preferential cell death mechanism. These authors also showed

that nsPEF-induced cell death was cell type specific, since HEK 293 cells and K562 cells underwent PAR-associated regulated necrosis in the presence of calcium, while Jurkat cells underwent apoptosis regardless of the presence or absence of calcium.

The production of reactive oxygen species (ROS) and subsequent DNA damage has also been proposed as a possible effect causing apoptosis [126]. NsPEFs do increase intracellular ROS, but it is not clear that this has significant effects on cell viability [127]. There is evidence that nsPEF stimulation with multiple, intense pulses causes damage to DNA or other critical proteins. Studies by comet assay have shown that significant DNA damage does occur very quickly after treatment (90-s posttreatment) with nsPEFs [128]. Some DNA repair was observed when permeabilization of cells for the comet assay was delayed for an hour. At this time it is not known if DNA damage is a primary (direct) effect of intense nanosecond electric fields or a secondary effect caused by membrane permeabilization and/or mediated by apoptosis-inducing factor (AIF) released from mitochondria or following caspase cleavage of DNA. A more detailed discussion on cell death mechanisms is given in Sect. 4.10 by S. Beebe.

Since earth life forms did not evolve in the presence of nsPEFs, it was of interest to determine what cellular systems would function in response to nsPEFs. It has been shown that cellular response to nsPEFs is distinct from those induced by previously known forms of cellular stress such as the protein-unfolding response, UV radiation, and heat [129]. A more specific discussion of these finding will be presented in the chapter by K Yano.

The research on cell death caused by nanosecond pulses has triggered studies on its application for cancer treatment. First studies [112] indicated the potential of such pulses for the controlled destruction of tumor tissue. Tumors were grown in flanks of mice and removed and treated ex vivo. In the first rudimentary experiments treating tumors in vivo using electrodes with two needles, tumor growth was decreased by 60 %. When treatment regimens and electrode designs were optimized, B16f10 melanoma [130] and hepatocellular tumors in mice [131] and rats [132] were eliminated by 75–100 %. These early studies have now led to the development of therapeutic methods for cancer treatment, particularly treatment of skin cancer [133–135]. This topic is described in detail in Sect. 5.12 by R. Nuccitelli.

### *1.3.3 New Research Directions*

#### 1.3.3.1 From Nanosecond to Picosecond Pulses

By reducing the duration of electric pulses from microseconds into the nanosecond range, the electric field–cell interactions shift increasingly from the plasma (cell) membrane to subcellular structures. Yet another domain of pulsed electric field interactions with cell structures and functions opens when the pulse duration is

reduced to values such that membrane charging becomes negligible, and direct electric field-molecular effects determine biological mechanisms. For dominance of such effects, the pulse duration needs to be less than the dielectric relaxation time of the cytoplasm. For mammalian cells, this holds for pulse duration of less than 1 ns.

The practical reason for entering this new field of bioelectrics by moving into the subnanosecond range is the possible use of antennas as pulse delivery systems instead of needle electrodes as well as the opportunity to observe direct electric field effects on biological mechanisms. These antenna systems are mainly based on the use of a prolate spheroidal reflector, where the pulse is launched from one focal point and reflected into a second focal point [77]. The use of needle or plate electrodes in therapeutic applications which rely on electroporation [136] or nanosecond pulsed electric fields (nsPEF) [133] requires that the electrodes are brought into close contact with the treated tissue. This limits the application to treatments of tissue close to the skin or surface of the body or by using invasive procedures or minimally invasive procedures by laparoscopy to treat internal organs. The use of antennas, on the other hand, would allow one to apply such electric fields to tissues (tumors) that are not easily accessible with needles. Also, focusing electrical energy on the target would reduce the damage to the tissue layers surrounding the target and the skin.

#### 1.3.3.2 From Membranes to Proteins

Most, if not all, effects of electric fields are analyzed in terms of electrical charging of plasma membranes and/or subcellular membranes. Since nsPEFs are extensions of classical electroporation, which was developed for permeabilization of plasma membranes for drug or nucleotide delivery to cells, the focus with submicrosecond pulses has remained on lipid bilayers for electric field effects. Although cellular plasma membranes include integral and peripheral proteins, these structures have generally been ignored because of their complexity compared to lipid bilayers. Only a few experimental analyses have approached the subject of electric field effects on proteins.

Initial studies with submicrosecond pulses demonstrated effects that breached membranous intracellular vesicles in human eosinophils [77]. Yet caution was exercised not to assume all cell responses would be exclusively on membranes. The intracellular effects were referred to as “intracellular electromanipulation” instead of “intracellular electroporation/permeabilization.” Beyond consideration for membrane effects, nsPEFs have been considered for possible effect on DNA [112, 115, 133]. However it is presently unclear if observed effects on DNA damage are due to direct, primary electric field effects or if they are secondary to intracellular assaults on upstream biological mechanisms that lead to DNA damage. More specifically, it is debated whether nsPEFs deliver sufficient energy, power, or high-frequency components to disrupt molecular bonding such as hydrogen bonding that contributes to the structure and stability of DNA or such bonding in

proteins. However, there are several simulation studies using molecular dynamics (MD) suggesting that nsPEFs can affect protein structure and at least one experimental study showing that nsPEFs can directly affect the catalytic activity of a protein kinase.

Using MD, high-intensity nsPEFs were found to cause a marked structural rearrangement along the major geometrical axis of the protein myoglobin [137]. In other MD studies, nsPEFs caused the soybean hydrophobic protein, a well-studied food protein, to unfold and lose all secondary structure [138]. Similar conclusions were reached for static and oscillating effects of nanosecond pulses that destabilized the structure of the insulin β-chain (30 amino acids) [139]. In a study with the human aquaporin four channel, nsPEFs were shown to switch the dipolar orientation of the histidine-201 residue [140]. However, it needs to be noted that except for the last study where 50- and 100-ns pulses at 650 kV/cm were applied, the assumed pulsed electric field amplitudes were in several MV/cm range, although for shorter pulse durations. Such pulse amplitudes are not realistic when considering the state of present pulse power technology.

However, both direct and indirect experimental evidence indicate that effects on proteins are likely occurring at much lower electric fields. NsPEFs were shown to have direct effects on the phosphotransferase activity of the catalytic subunit of the cAMP-dependent protein kinase (PKA) [122]. NsPEFs caused a 41 % and 45 % loss in catalytic activity with one and ten pulses at 60 ns, 60 kV/cm, respectively, and a 55 % and 77 % activity loss for one and ten pulses at 300 ns, 26 kV/cm, respectively. Given that the one pulse and ten pulse conditions between 60 ns, 60 kV/cm and 300 ns, 26 kV/cm exhibited similar energy densities (1.7 J/cc), the inhibitory effects on kinase structure/function appear to be, at least in part, not to scale with energy density. This is consistent with effects of nsPEFs on nsPEF-induced cytochrome *c* release and caspase activity in intact cells [112, 113]. These studies further indicate that nsPEF-induced inactivation of kinase activity is due, at least in part, to charging effects transferred to the enzyme rather than energy deposition.

Also, observations that nsPEFs induce $Ca^{2+}$-dependent dissipation of the mitochondria membrane potential ($\Delta\Psi m$), which is enhanced when high-frequency components are present in fast rise-fall waveforms, suggest events that are not due to permeabilization of the inner mitochondrial membrane; plasma membrane poration (and thereby intracellular membranes) is not $Ca^{2+}$ dependent. Since all $Ca^{2+}$-mediated events require proteins, it is possible that nsPEFs affect a protein(s) or protein complex that changes the transmembrane voltage, thereby leading to opening the mitochondrial permeability transition pore (mPTP) [81, 85]. Effects of nsPEFs on proteins open a new paradigm for electric field effects on cell structures and functions.

#### 1.3.3.3 Thermally Assisted Electroeffects

Thermal effects, although generally avoided in bioelectric studies, have their place in bioelectrics, even for pulses short compared to the dielectric relaxation time of

the membrane. Simultaneously pulsing and heating cells, either by utilizing the Joule heat generated through high repetition rate pulsing [141] or using pulse-independent methods such as microwave heating, allow us to reduce the electrical energy required for inducing cell death by a considerable amount. This has been shown recently in a study where 200-ps long pulses were applied to a slightly heated cell suspension [142] Cell death, as recorded by means of trypan blue uptake, increased considerably for heating above physiological temperature. The results indicate that thermal assistance of electro-technologies, such as tumor ablation and gene therapy, will allow us to reduce the electrical energy (pulse amplitude) and consequently reduce tissue damage.

#### 1.3.3.4 Nonthermal Plasmas for Environmental and Medical Applications

A fascinating new field of research using pulsed electric fields to generate nonthermal plasma is plasma medicine [143, 144]. Plasma reactors for environmental and medical applications have found their place in "bioelectrics." Again, as in the field of bioelectrics as discussed in this chapter, nanosecond pulses play a major role. Experimental studies with nonequilibrium gliding gas discharges have shown their potential for environmental and medical applications, such as chemical and bacterial decontamination [145].

## References

1. Neumann, E., Schaefer-Ridder, M., Wang, Y., Hofschneider, P.H.: Gene transfer into mouse lyoma cells by electroporation in high electric fields. EMBO J. **1**, 841–845 (1982)
2. Wong, T.K., Neumann, E.: Electric field mediated gene transfer. Biophys. Biochem. Res. Commun. **107**, 584–587 (1972)
3. Neumann, E., Rosenheck, K.: Permeability changes induced by electric impulses in vesicular membranes. J. Membr. Biol. **10**, 279–290 (1972)
4. Neumann, E., Gerisch, G., Opatz, K.: Cell fusion induced by high electric impulses applied to Dictostelium. Naturwissenschaften **67**, 414–415 (1980)
5. Eisenstein, M.: A look back: a shock to the system. Nat. Methods **3**, 66 (2006)
6. Griese, T., Kakorin, S., Neumann, E.: Conductometric and electrooptic relaxation spectrometry of lipid vesicle electroporation at high fields. Phys. Chem. Chem. Phys. **4**, 1217–1227 (2002)
7. Schmeer, M., Seipp, T., Pliquett, U., Kakorin, S., Neumann, E.: Mechanism the conductivity changes caused by membrane electroporation of CHO cell-pellets. Phys. Chem. Chem. Phys. **6**, 5564–5574 (2004)
8. Pliquett, U., Gallo, S., Hui, S.W., Gusbeth, C., Neumann, E.: Local a transient structural changes in stratum corneum at high electric fields: Contribution of Joule heating. Bioelectrochemistry **67**, 37–46 (2005)
9. Neumann, E., Kakorin, S.: Electroporation of curved lipid membranes in ionic strength gradients. Biophys. Chem. **85**, 249–271 (2000)

10. Kakorin, S., Redeker, E., Neumann, E.: Electroporative deformation of salt filled vesicles. Eur. Biophys. J. **27**, 43–53 (1998)
11. Neumann, E., Tönsing, K., Kakorin, S., Budde, P., Frey, J.: Mechanism of electroporative dye uptake by mouse B cells. Biophys. J. **74**, 98–108 (1998)
12. Dimitrov, V., Kakorin, S., Neumann, E.: Transient Oscillation of shape and membrane conductivity changes by field pulse-induced electroporation in nano-sized phospholipid vesicles. Phys. Chem. Chem. Phys. **15**, 6303–6632 (2013)
13. Abidor, I. G., Arakelyan, V. B., Chernomordik, L. V., Chizmadzhev, Y. A., Pastuchenko, V. P., Tarasevich, M. R.: Electric Breakdown of Bilayer Lipid Membrane. I. The main experimental facts and their theoretical discussion, Bioelectrochem. Bioenerg. **6**, 37–52. (1979)
14. Andre, F.M., Gehl, J., Sersa, G., Preat, V., Hojman, P., Eriksen, J., Golzio, M., Cemazar, M., Pavselj, N., Rols, M.-P., Miklavcic, D., Neumann, E., Teissie, J., Mir, L.M.: Efficiency of high- and low voltage pulse combinations for gene electrotransfer in muscle liver, tumor, and skin. Hum. Gene Ther. **19**, 1261–1271 (2008)
15. Neumann, E.: The relaxation hysteresis of membrane electroporation. In: Neumann, E., Sowers, A.E., Jordan, C.A. (eds.) Electroporation and Electrofusion in Cell Biology, pp. 61–82. Plenum Press, New York (1989)
16. Neumann, E., Kakorin, S., Toensing, K.: Fundamentals of electroporative delivery of drugs and genes. Bioelectrochem. Bioenerg. **48**, 3–1 (1999)
17. Coster, H.G.: A quantitative analysis of the voltage-current relationships of fixed charge membranes and the associated property of "punch-through". Biophys. J. **5**(5), 669–686 (1965)
18. Sale, A.J.H., Hamilton, W.A.: Effects of high electric fields on microorganisms: I. Killing of bacteria and yeasts. Biochim. Biophys. Acta Gen. Subj. **148**(3), 781–788 (1967)
19. Sale, A.J.H., Hamilton, W.A.: Effects of high electric fields on micro-organisms: III. Lysis of erythrocytes and protoplasts. Biochim. Biophys. Acta Biomembr. **163**(1), 37–43 (1968)
20. Pohl, H.A., Crane, J.S.: Dielectrophoresis of cells. Biophys. J. **11**(9), 711–727 (1971)
21. Crowley, J.M.: Electrical breakdown of bimolecular lipid membranes as an electromechanical instability. Biophys. J. **13**(7), 711–724 (1973)
22. Zimmermann, U., Pilwat, G., Riemann, F.: Dielectric breakdown of cell membranes. Biophys. J. **14**(11), 881–899 (1974)
23. Largus, S. 47. Compositiones Medicae. Quoted in Kellaway, P.: The part played by electric fish in the early history of bioelectricity and electrotherapy. Bull. Hist. Med. **20**, 112–137 (1946)
24. Jallabert, J.: Experiences sur l'electricite avec quelques conjectures sur la cause de ses effets. http://catalogue.bnf.fr/ark:/12148/cb393088488 (1746)
25. Franklin, B: Letters to Peter Collison (1749). In: Labaree, L. W. (ed.) The Papers of Benjamin Franklin, vol. 3, January 1, 1745, through June 30, 1750, pp 391–393. Yale University Press, New Haven (1961)
26. Nollet, J. A.: Recherches sur les causes particulieres des phénoménes électriques, et sur les effets nuisibles ou avantageux qu'on peut en attendre. Nouv. éd. Paris, Guerin u. Delatour (1754)
27. Galvani, L.: Aloysii Galvani De viribus electricitatis in motu musculari commentarius, Ex Typographia Instituti Scientiarium (1791)
28. Mauduyt de la Varenne, P.J.C. Mémoire sur les différentes manières d'administrer l'électricité, et observations sur les effets qu'elles ont produits. Paris. l'Imprimerie Royale. (1784)
29. Pauly, H., Schwan, H.P.: Impedance of a suspension of ball-shaped particles with a shell; a model for the dielectric behavior of cell suspensions and protein solutions. Z Naturforsch B **14B**, 125–131 (1959)
30. Hamilton, W.A., Sale, A.J.H.: Effects of high electric fields on microorganisms II. Mechanism of action of the lethal effect. Biochim. Biophys. Acta **148**, 789–800 (1967)

31. Kinosita Jr., K., Tsong, T.Y.: Hemolysis of human erythrocytes by transient electric field. Proc. Natl. Acad. Sci. U. S. A. **74**, 1923–1927 (1977)
32. Senda, M., Takeda, J., Abe, S., Nakamura, T.: Induction of cell fusion of plant protoplasts by electrical stimulation. Plant Cell Physiol. **20**, 1441–1443 (1979)
33. Scheurich, P., Zimmermann, U.: Electrically stimulated fusion of different plant cell protoplasts: mesophyll cell and guard cell protoplasts of *Vicia faba*. Plant Physiol. **67**, 849–853 (1981)
34. Teissie, J., Tsong, T.Y.: Electric field induced transient pores in phospholipid bilayer vesicles. Biochemistry **20**, 1548–1554 (1981)
35. Gordon, P.B., Seglen, P.O.: Autophagic sequestration of [$^{14}$C]sucrose, introduced into rat hepatocytes by reversible electro-permeabilization. Exp. Cell Res. **142**, 1–14 (1982)
36. Teissie, J., Knutson, V.P., Tsong, T.Y., Lane, M.D.: Electric pulse-induced fusion of 3T3 cells in monolayer culture. Science **216**, 537–538 (1982)
37. Potter, H., Weir, L., Leder, P.: Enhancer-dependent expression of human kappa immunoglobulin genes introduced into mouse pre-B lymphocytes by electroporation. Proc. Natl. Acad. Sci. U. S. A. **81**, 7161–7165 (1984)
38. Sugar, I.P., Neumann, E.: Stochastic model for electric field-induced membrane pores. Electroporation. Biophys. Chem. **19**, 211–225 (1984)
39. Lo, M.M., Tsong, T.Y., Conrad, M.K., Strittmatter, S.M., Hester, L.D., Snyder, S.H.: Monoclonal antibody production by receptor-mediated electrically induced cell fusion. Nature **310**(5980), 792–794 (1984)
40. Okino, M., Mohri, H.: Effects of a high-voltage electrical impulse and an anticancer drug on in vivo growing tumors. Jap. J. Cancer Res. **78**, 1319–1321 (1987)
41. Mir, L.M., Banoun, H., Paoletti, C.: Introduction of definite amounts of nonpermeant molecules into living cells after electropermeabilization: direct access to the cytosol. Exp. Cell Res. **175**, 15–25 (1988)
42. Sersa, G., Cemazar, M., Miklavcic, D.: Antitumor effectiveness of electrochemotherapy with cis-diamminedichloroplatinum(II) in mice. Cancer Res. **55**, 3450–3455 (1995)
43. Gilbert, R., Jaroszeski, M.J., Heller, R.: Novel electrode designs for electrochemotherapy. Biochemica Biophysica Acta **1334**, 9–14 (1997)
44. Frandsen, S.K., Gissel, H., Hojman, P., Tramm, T., Eriksen, J., Gehl, J.: Direct therapeutic applications of calcium electroporation to effectively induce tumor necrosis. Cancer Res. **72**, 1336–1341 (2012)
45. Mir, L.M., Belehradek, M., Domenge, C., Orlowski, S., Poddevin, B., Belehradek Jr., J., Schwaab, G., Luboinski, B., Paoletti, C.: Electrochemotherapy, a new antitumor treatment: first clinical trial. C. R. Acad. Sci. III **313**, 613–618 (1991)
46. Titomirov, A.V., Sukharev, S., Kistanova, E.: In vivo electroporation and stable transformation of skin cells of newborn mice by plasmid DNA. Biochim. Biophys. Acta **1088**, 131–134 (1991)
47. Heller, R., Jaroszeski, M., Atkin, A., Moradpour, D., Gilbert, R., Wands, J., Nicolau, C.: In vivo gene electroinjection and expression in rat liver. FEBS Lett. **389**, 225–228 (1996)
48. Rols, M.P., Delteil, C., Golzio, M., Dumond, P., Cros, S., Teissie, J.: In vivo electrically mediated protein and gene transfer in murine melanoma. Nat. Biotechnol. **16**, 168–171 (1998)
49. Aihara, H., Miyazaki, J.: Gene transfer into muscle by electroporation in vivo. Nat. Biotechnol. **16**, 867–870 (1998)
50. Daud, A.I., DeConti, R.C., Andrews, S., Urbas, P., Riker, A.I., Sondak, V.K., Munster, P.N., Sullivan, D.M., Ugen, K.E., Messina, J.L., Heller, R.: Phase I trial of interleukin-12 plasmid electroporation in patients with metastatic melanoma. J. Clin. Oncol. **26**, 5896–5903 (2008)
51. Prausnitz, M.R., Bose, V.G., Langer, R., Weaver, J.C.: Electroporation of mammalian skin: a mechanism to enhance transdermal drug delivery. Proc. Natl. Acad. Sci. U. S. A. **90**(22), 10504–10508 (1993)
52. Prausnitz, M.R., Lau, B.S., Milano, C.D., Conner, S., Langer, R., Weaver, J.C.: A quantitative study of electroporation showing a plateau in net molecular transport. Biophys. J. **65**, 414–422 (1993)

53. Davalos, R.V., Mir, L., Rubinsky, B.: Tissue ablation with irreversible electroporation. Ann. Biomed. Eng. **33**(2), 223–231 (2005)
54. Grasso, R.J., Heller, R., Cooley, J.C., Haller, E.M.: Electrofusion of individual animal cells directly to intact corneal epithelial tissue. Biochim. Biophys. Acta **980**(1), 9–14 (1989)
55. Heller, R., Grasso, R.J.: Transfer of human membrane surface components by incorporating individual human cells into intact animal tissue by cell-tissue electrofusion *in vivo*. Biochim. Biophys. Acta **1024**, 185–188 (1990)
56. Garcia, P.A., Davalos, R.V., Miklavcic, D.: A numerical investigation of the electric and thermal cell kill distributions in electroporation-based therapies in tissue. PLoS One **9**(8), e103083 (2014)
57. Poo, M., Robinson, K.R.: Electrophoresis of concanavalin A receptors along embryonic muscle cell membrane. Nature **265**(5595), 602–605 (1977)
58. Pucihar, G., Miklavcic, D., Kotnik, T.: A time-dependent numerical model of transmembrane voltage inducement and electroporation of irregularly shaped cells. IEEE Trans. Biomed. Eng. **56**(5), 1491–1501 (2009)
59. Rols, M.P., Delteil, C., Golzio, M., Teissié, J.: Control by ATP and ADP of voltage-induced mammalian-cell-membrane permeabilization, gene transfer and resulting expression. Eur. J. Biochem. **254**(2), 382–388 (1998)
60. Pucihar, G., Kotnik, T., Miklavcic, D., Teissié, J.: Kinetics of transmembrane transport of small molecules into electropermeabilized cells. Biophys. J. **95**(6), 2837–2848 (2008)
61. Huynh, C., Roth, D., Ward, D.M., Kaplan, J., Andrews, N.W.: Defective lysosomal exocytosis and plasma membrane repair in Chediak-Higashi/beige cells. Proc. Natl. Acad. Sci. U. S. A. **101**(48), 16795–16800 (2004)
62. Neil, G.A., Zimmermann, U.: Electrofusion. Methods Enzymol. **220**, 174–196 (1993)
63. NICE interventional procedures guidance [IPG478] (2014)
64. Broderick, K.E., Humeau, L.M.: Electroporation-enhanced delivery of nucleic acid vaccines. Expert Rev. Vaccines **14**(2), 195–204 (2015)
65. Pavlin, D., Cemazar, M., Sersa, G., Tozon, N.: IL-12 based gene therapy in veterinary medicine. J. Transl. Med. **10**, 234 (2012)
66. Heller, L.C., Heller, R.: In vivo electroporation for gene therapy. Hum. Gene Ther. **17**(9), 890–897 (2006)
67. Heller, R., Heller, L.C.: Gene electrotransfer clinical trials. Adv. Genet. **89**, 235–262 (2015)
68. Young, J.L., Dean, D.A.: Electroporation-mediated gene delivery. Adv. Genet. **89**, 49–88 (2015)
69. Puértolas, E1., Luengo, E., Álvarez, I., Raso, J.: Improving mass transfer to soften tissues by pulsed electric fields: fundamentals and applications. Annu. Rev. Food Sci. Technol. **3**, 263–282 (2012)
70. Rieder, A., Schwartz, T., Schön-Hölz, K., Marten, S.M., Süss, J., Gusbeth, C., Kohnen, W., Swoboda, W., Obst, U., Frey, W.: Molecular monitoring of inactivation efficiencies of bacteria during pulsed electric field treatment of clinical wastewater. J. Appl. Microbiol. **105**(6), 2035–2045 (2008)
71. Dower, W.J., Miller, J.F., Ragsdale, C.W.: High efficiency transformation of E. coli by high voltage electroporation. Nucleic Acids Res. **16**(13), 6127–6145 (1988)
72. Miller, J.F., Dower, W.J., Tompkins, L.S.: High-voltage electroporation of bacteria: genetic transformation of Campylobacter jejuni with plasmid DNA. Proc. Natl. Acad. Sci. U. S. A. **85**(3), 856–860 (1988)
73. Meilhoc, E1., Masson, J.M., Teissié, J.: High efficiency transformation of intact yeast cells by electric field pulses. Biotechnology (N Y) **8**(3), 223–227 (1990)
74. Brown, L.E., Sprecher, S.L., Keller, L.R.: Introduction of exogenous DNA into Chlamydomonas reinhardtii by electroporation. Mol. Cell. Biol. **11**(4), 2328–2332 (1991)
75. Trick, H.N., Bates, G.W.: Electrofusion of plant protoplasts. Selection and screening for somatic hybrids of Nicotiana. Methods Mol. Biol. **55**, 165–179 (1995)

76. Staempfli, R.: Reversible breakdown of the excitable membrane of a ranvier node. An. Acad. Bras. Ciências **30**, 57 (1958)
77. Schoenbach, K.H., Beebe, S.J., Buescher, E.S.: Intracellular effect of ultrashort electrical pulses. J. Bioelectromagnetics **22**, 440–448 (2001)
78. Kolb, J.F., Kono, S., Schoenbach, K.H.: Nanosecond pulsed electric field generators for the study of subcellular effects. Bioelectromagnetics J. **27**, 172–187 (2006)
79. Xiao, S., Altunc, S., Kumar, P., Baum, C.E., Schoenbach, K.H.: A reflector antenna for focusing in the near field. IEEE Antennas Wirel. Propag. Lett. **9**, 12–15 (2010)
80. Schoenbach, K.H., Joshi, R.P., Kolb, J.F., Chen, N., Stacey, M., Blackmore, P.F., Buescher, E.S., Beebe, S.J.: Ultrashort electrical pulses open a new gateway into biological cells. Proc. IEEE **92**, 1122–1137 (2004)
81. Joshi, R.P., Hu, Q., Schoenbach, K.H.: Modeling studies of cell response to ultrashort high-intensity electric fields – implications for intracellular manipulation. IEEE Trans. Plasma Sci. **32**, 1677–1686 (2004)
82. Schoenbach, K.H., Hargrave, B., Joshi, R.P., Kolb, J.F., Osgood, C., Nuccitelli, R., Pakhomov, A., Swanson, R.J., Stacey, M., White, J.A., Xiao, S., Zhang, J., Beebe, S.J., Blackmore, P.E., Buescher, E.S.: Bioelectric effects of nanosecond pulses. IEEE Trans. Diel. Electr. Insul. **14**, 1088–1119 (2007)
83. Smith, K.C., Gowrishankar, T.R., Esser, A.T., Stewart, D.A., Weaver, J.C.: The spatially distributed dynamic transmembrane voltage of cells and organelles due to 10 ns pulses: meshed transport networks. IEEE Trans. Plasma Sci. **34**, 1394–1404 (2006)
84. Stewart, D.A., Gowrishankar, T.R., Weaver, J.C.: Three dimensional transport lattice model for describing action potentials in axons stimulated by external electrodes. Bioelectrochemistry **69**, 88–93 (2006)
85. Weaver, J.C.: Harvard-MIT Division of Health Sciences and Technology, Cambridge, MA 02139, USA, private communication (2006)
86. Gowrishankar, T.R., Esser, A.T., Vasilkoski, Z., Smith, K.C., Weaver, J.C.: Microdosimetry for conventional and supra-electroporation in cells with organelles. BBRC **341**, 1266–1276 (2006)
87. Schoenbach, K.H., Katsuki, S., Stark, R.H., Buescher, E.S., Beebe, S.J.: Bioelectrics – new applications for pulsed power technology. IEEE Trans. Plasma Sci. **30**, 293–300 (2002)
88. Kotnik, T., Miklavcic, D.: Theoretical evaluation of voltage inducement on internal membranes of biological cells exposed to electric fields. Biophys. J. **90**, 480–491 (2006)
89. Kakorin, E., Redeker, E., Neumann, E.: Electroporative deformation of salt filled lipid vesicles. Eur Biophys **J27**, 43–53 (1998)
90. Frey, W., White, J.A., Price, R.O., Blackmore, P.F., Joshi, R.P., Nuccitelli, R., Beebe, S.J., Schoenbach, K.H., Kolb, J.F.: Plasma membrane voltage changes during nanosecond pulsed electric field exposure. Biophys. J. **90**, 3608–3615 (2006)
91. Vasilkoski, Z., Esser, A.T., Gowrishankar, T.R., Weaver, J.C.: Membrane electroporation: the absolute rate equation and nanosecond time scale pore creation. Phys. Rev. **E74**, 021904-1–021904-12 (2006)
92. Pakhomov, A.G., Shevin, R., White, J., Kolb, J.F., Pakhomova, O.N., Joshi, R.P., Schoenbach, K.H.: Membrane permeabilization and cell damage by ultrashort electric field shocks. Arch. Biochem. Biophys. **465**(1), 109–118 (2007)
93. Halestrap, A.P., McStay, G.P., Clarce, S.J.: The permeability transition pore complex: another view. Biochimie **84**, 153–166 (2002)
94. Tieleman, D., Leontiadou, H., Mark, A.E., Marrink, S.J.: Simulation of pore formation in lipid bilayers by mechanical stress and electric fields. J. Am. Chem. Soc. **125**, 6382–6383 (2003)
95. Vernier, P.T., Ziegler, M.J., Sun, Y., Gundersen, M.A., Tieleman, T.P.: Nanopore-facilitated, voltage-driven translocation in lipid bilayers – in cells and in silico. Phys. Biol. **3**, 233–247 (2005)

96. Vernier, P.T., Ziegler, M.J., Sun, Y., Chang, W.V., Gundersen, M.A., Tieleman, D.P.: Nanopore formation and phosphatidylserine externalization in a phospholipid bilayer at high transmembrane potential. J. Am. Chem. Soc. **128**, 6288–6289 (2006)
97. Schoenbach, K.H., Baum, C.E., Joshi, R.P., Beebe, S.J.: A scaling law for membrane permeabilization with nanopulses. Special issue on Bioelect. IEEE Trans. Dielect. Elect. Insulation. **16**, 1224–1235 (2009a)
98. Pakhomov, A.G., Semenov, I., Xiao, S., Pakhomova, O.N., Gregory, B., Schoenbach, K.H., Ullery, J.C., Beier, H.T., Rajulapati, S.R., Ibey, B.L.: Cancellation of cellular responses to nanoelectroporation by reversing the stimulus polarity. Cell. Mol. Life Sci. **71**(22), 4431–4441 (2014)
99. Schoenbach, K.H., Pakhomov, A.G., Semenov, I., Xiao, S., Pakhomova, O.N., Ibey, B.L.: Ion transport into cells exposed to monopolar and bipolar nanosecond pulses. Bioelectrochemistry **103**, 44–51 (2015)
100. Schoenbach, K.H., Peterkin, F.E., Alden, R.W., Beebe, S.J.: The effect of pulsed electric fields on biological cells: experiments and applications. Trans. Plasma Sci. **25**, 284–292 (1997)
101. Schoenbach, K.H., Joshi, R.P., Stark, R.H., Dobbs, F., Beebe, S.J.: Bacterial decontamination of liquids with pulsed electric fields. IEEE Trans Dielect. Electr. Insul. **7**, 637–645 (2000)
102. Berridge, M.J., Bootman, M.D., Lipp, P.: Calcium – a life and death signal. Nature **395**, 645–648 (1998)
103. Susin, S.A., Zamzami, N., Kroemer, G.: Mitochondria as regulators of apoptosis: doubt no more. Biochim. Biophys. Acta **1366**, 151–165 (1998)
104. Buescher, E.S., Schoenbach, K.H.: Effects of submicrosecond, high intensity pulsed electric fields on living cells – intracellular electromanipulation. IEEE Trans Dielect. Electr. Insul. **10**, 788–794 (2003)
105. Ghazala, A., Schoenbach, K.H.: Biofouling prevention with pulsed electric fields. IEEE Trans. Plasma Sci. **28**, 115–121 (2000)
106. Vernier, P.T., Sun, Y., Marcu, L., Salemi, S., Craft, C.M., Gundersen, M.A.: Calcium bursts induced by nanosecond electrical pulses. BBRC **310**, 286–295 (2003)
107. Vernier, P.T., Sun, Y., Marcu, L., Craft, C.M., Gundersen, M.A.: Nanoelectropulse-induced phosphatidylserine translocation. Biophys. J. **86**, 4040–4048 (2004)
108. Beebe, S.J., White, J.A., Blackmore, P.F., Deng, Y., Somers, K., Schoenbach, K.H.: Diverse effects of nanosecond pulsed electric fields on cells and tissues. DNA Cell Biol. **22**, 785–796 (2003)
109. White, J.A., Blackmore, P.F., Schoenbach, K.H., Beebe, S.J.: Stimulation of capacitive calcium entry in HL-60 cells by nanosecond pulsed electric fields (nsPEF). J. Biol. Chem. **279**, 22964–22972 (2004)
110. Zhang, J., Blackmore, P.F., Hargrave, B.Y., Xiao, S., Beebe, S.J., Schoenbach, K.H.: The characteristics of nanosecond pulsed electrical field stimulation on platelet aggregation in vitro. Arch. Biochem. Biophys. **471**, 240–248 (2008)
111. Galluzzi, L., Bravo-San Pedro, J.M., Vitale, I., Aaronson, S.A., Abrams, J.M., Adam, D., et al.: Essential versus accessory aspects of cell death: recommendations of the NCCD 2015. Cell Death Differ. (2014). doi:10.1038/cdd.2014.137
112. Beebe, S.J., Fox, P.M., Rec, L.C., Somers, K., Stark, R.H., Schoenbach, K.H.: Nanosecond Pulsed Electric Field (nsPEF) effects on cells and tissues: apoptosis induction and tumor growth inhibition. IEEE Trans. Plasma Sci. **30**, 286–292 (2002)
113. Beebe, S.J., Fox, P.M., Rec, L.J., Willis, L.K., Schoenbach, K.H.: Nanosecond, high intensity pulsed electric fields induce apoptosis in human cells. FASEB J. **17**, 1493 (2003)
114. Vernier, P.T., Li, A., Marcu, L., Craft, C.M., Gundersen, M.A.: Ultrashort pulsed electric fields induce membrane phospholipid translocation and caspase activation: differential sensitivities of jurkat T lymphoblasts and rat glioma C6 cells. IEEE Trans. Diel. Electr. Insul. **10**, 795–809 (2003)

115. Stacey, M., Stickley, J., Fox, P., Statler, V., Schoenbach, K.H., Beebe, S.J., Buescher, S.: Differential effects in cells exposed to ultra-short, high intensity electric fields: cell survival, DNA damage, and cell cycle analysis. Mutat. Res. **542**, 65–75 (2003)
116. Müller, A., Günther, D., Düx, F., Naumann, M., Meyer, T.F., Rudel, T.: Neisseria porin (PorB) causes rapid calcium influx in target cells and induces apoptosis by the activation of cysteine proteases. EMBO J. **18**, 339–352 (1999)
117. Savill, J., Haslett, C.: Granulocyte clearance by apoptosis in the resolution of inflammation. Semin. Cell Biol. **6**, 385–360 (1995)
118. Tsujimot, Y., Shimizu, S.: The voltage-dependent anion channel: an essential player in apoptosis. Biochimie **84**, 187–193 (2002)
119. Weaver, J.C.: Electroporation of biological membranes from multicellular to nanoscales. IEEE Trans. Diel. Electr. Insul. **10**, 754–768 (2003)
120. Beebe, S.J., Chen, Y.J., Sain, N.M., Schoenbach, K.H., Xiao, S.: Transient features in nanosecond pulsed electric fields differentially modulate mitochondria and viability. PLoS One **7**, e51349 (2012)
121. Beebe, S.J., Sain, N.M., Ren, W.: Induction of cell death mechanisms and apoptosis by nanosecond pulsed electric fields (nsPEFs). Cells **2**, 136–162 (2013)
122. Beebe, S.J.: Considering effects of nanosecond pulsed electric fields on proteins. Bioelectrochemistry **S1567–5394**(14), 00130–00133 (2014). doi:10.1016/j.bioelechem.2014.08.014
123. Morotomi-Yano, K., Akiyama, H., Yano, K.: Different involvement of extracellular calcium in two modes of cell death induced by nanosecond pulsed electric fields. Arch. Biochem. Biophys. **555–556**, 47–54 (2014)
124. Ford, W.E., Ren, W., Blackmore, P.F., Schoenbach, K.H., Beebe, S.J.: Nanosecond pulsed electric fields stimulate apoptosis without release of pro-apoptotic factors from mitochondria in B16f10 melanoma. Arch. Biochem. Biophys. **497**, 82–89 (2010)
125. Ren, W., Beebe, S.J.: An apoptosis targeted stimulus with nanosecond pulsed electric fields (nsPEFs) in E4 squamous cell carcinoma. Apoptosis **16**, 382–393 (2011)
126. Walker III, K., Pakhomova, O.N., Kolb, J.F., Schoenbach, K.H., Stuck, B.E., Murphy, M.R., Pakhomov, A.G.: Oxygen enhances lethal effect of high-intensity, ultrashort electrical pulses. Bioelectromagnetics J. **27**, 221–225 (2006)
127. Pakhomova, O.N1., Khorokhorina, V.A., Bowman, A.M., Rodaitė-Riševičienė, R., Saulis, G., Xiao, S., Pakhomov, A.G.: Oxidative effects of nanosecond pulsed electric field exposure in cells and cell-free media. Arch. Biochem. Biophys. **527**(1), 55–64 (2012)
128. Nuccitelli, R., Chen, X., Pakhomov, A.G., Baldwin, W.H., Sheikh, S., Pomicter, J.L., Ren, W., Osgood, C., Swanson, R.J., Kolb, J.F., Beebe, S.J., Schoenbach, K.H.: A new pulsed electric field therapy for melanoma disrupts the tumor's blood supply and causes complete remission without recurrence. Int. J. Cancer **125**, 438–445 (2009)
129. Morotomi-Yano, K., Oyadomari, S., Akiyama, H., Yano, K.: Nanosecond pulsed electric fields act as a novel cellular stress that induces translational suppression accompanied by eIF2α phosphorylation and 4E-BP1 dephosphorylation. Exp. Cell Res. **318**, 1733–1744 (2012)
130. Chen, X., Kolb, J.F., Swanson, R.J., Schoenbach, K.H., Beebe, S.J.: Apoptosis initiation and angiogenesis inhibition: melanoma targets for nanosecond pulsed electric fields. Pigment Cell Melanoma Res. **23**, 554–563 (2010)
131. Chen, X., Zhuang, J., Kolb, J.F., Schoenbach, K.H., Beebe, S.J.: Long term survival of mice with hepatocellular carcinoma after pulse power ablation with nanosecond pulsed electric fields. Technol. Cancer Res. Treat. **11**, 83–93 (2012)
132. Chen, R., Sain, N.M., Harlow, K.T., Chen, Y.J., Shires, P.K., Heller, R., Beebe, S.J.: A protective effect after clearance of orthotopic rat hepatocellular carcinoma by nanosecond pulsed electric fields. Eur. J. Cancer **50**, 2705–2713 (2014)

133. Nuccitelli, R.L., Pliquett, U., Chen, X., Ford, W., Swanson, R.J., Beebe, S.J., Kolb, J.F., Schoenbach, K.H.: Nanosecond Pulsed electric fields cause melanomas to self-destruct. Biochem. Biophys. Res. Commun. (BBRC) **343**, 351–360 (2006)
134. Nuccitelli, R., Tran, K., Athos, B., Kreis, M., Nuccitelli, P., Chang, K.S., Epstein Jr., E.H., Tang, J.Y.: Nanoelectroablation therapy for murine basal cell carcinoma. Biochem. Biophys. Res. Commun. **424**, 446–450 (2012)
135. Nuccitelli, R., Wood, R., Kreis, M., Athos, B., Huynh, J., Lui, K., Nuccitelli, P., Epstein Jr., E.H.: First-in-human trial of nanoelectroablation therapy for basal cell carcinoma: proof of method. Exp. Dermatol. **23**, 135–137 (2014)
136. Hofmann, G.A.: Instrumentation and electrodes for in vivo electroporation. In: Jaroszewski, M. J., Heller, R., Gilbert, R. (eds.) Electrochemotherapy, Electrogenetherapy, and Transdermal Drug Delivery, pp. 37–61. Humana Press, Totowa (2000)
137. Marracino, P., Apollonio, F., Liberti, M., d'Inzeo, G., Amadei, A.: Effect of high exogenous electric pulses on protein conformation: myoglobin as a case study. J. Phys. Chem. B **117**(8), 2273–2279 (2013)
138. Singh, A., Orsat, V., Raghavan, V.: Soybean hydrophobic protein response to external electric field: a molecular modeling approach. Biomolecules **3**, 168–179 (2013)
139. Budi, A., Legge, F.S., Treutlein, H., Yarovsky, I.: Electric field effects on insulin chain-B conformation. J. Phys. Chem. B **109**, 22641–22648 (2005)
140. Reale, R., English, N.J., Garate, J.A., Marracino, P., Liberti, M., Apollonio, F.: Human aquaporin 4 gating dynamics under and after nanosecond-scale static and alternating electric-field impulses: a molecular dynamics study of field effects and relaxation. J. Chem. Phys. **139**(20), 205101 (2013)
141. Xiao, S., Guo, S., Vasyl, N., Heller, R., Schoenbach, K.H.: Subnanosecond electrical pulses cause membrane permeabilization and cell death. IEEE Trans. Biomed. Eng. **58**, 1239–1245 (2011)
142. Camp, J.T., Jing, Y., Zhuang, J., Juergen, K., Beebe, S.J., Song, J., Joshi, R.P., Xiao, S., Schoenbach, K.H.: Cell death induced by subnanosecond pulsed electric fields at elevated temperatures. IEEE Trans. Plasma Sci **40**(10), 2334–2347 (2012)
143. Jiang, C., Chen, M.T., Gorur, A., Schaudinn, C., Jaramillo, D.E., Costerton, J.W., Sedghizadeh, P.P., Vernier, P.T., Gundersen, M.A.: Atmospheric-pressure cold plasma for endodontic disinfection. IEEE Trans. Plasma Sci. **37**, 1190–1195 (2009)
144. Kong, M.G., Groesen, G., Morfill, G., Nosenko, T., Shimizu, T., van Dijk, J., Zimmermann, J. L.: Plasma medicine: an introductory review. New J. Phys. **11**, 115012 (2009) (35 pp)
145. Malik, M.A., Jiang, C., Dhali, S.K., Heller, R., Schoenbach, K.H.: Coupled sliding discharges: a scalable nonthermal plasma system utilizing positive and negative streamers on opposite sides of a dielectric layer. Plasma Chem. Plasma Process. (2014). doi:10.1007/s11090-014-9528-2